

TECHNICAL REPORT 1866
August 2001

**COMWIN Antenna Project:
Fiscal Year 2001
Final Report**

R. C. Adams
R. S. Abramo
D. W. Von Mueller

Approved for public release;
distribution is unlimited.



SSC San Diego
San Diego, CA 92152-5001

SSC SAN DIEGO
San Diego, California 92152-5001

Ernest L. Valdes, CAPT, USN
Commanding Officer

R. C. Kolb
Executive Director

ADMINISTRATIVE INFORMATION

The work described in this report was performed for the Expeditionary Warfare Division of the Office of Naval Research (ONR 353) by the SSC San Diego Signal Processing & Communications Technology Branch (D855).

ACKNOWLEDGMENTS

We have the pleasure to acknowledge the assistance and hospitality of the Naval Health Research Center-Detachment at Brooks AFB in San Antonio, TX. Dr. John D'Andrea and particularly Dr. John Ziriak supervised the experiment and provided excellent support. We would also like to thank the other members of the team who worked hard to make the experiment a success. These include Don Hatcher, William Hurt, Duane Cox, and Donald Marchello. Wayne Hammer of SSC Charleston lent his experience and skill in measuring and assessing the radiation hazard of the vest and helmet antennas. Knowing that there is a problem is the first step in solving it.

We would also like to thank P. Michael McGinnis of SSC San Diego who provided support in developing the distribution network of the COMWIN system. We would also like to express our profound appreciation to Bob O'Neill, who has fabricated all the antennas for the COMWIN system. His artistry is exceeded only by his willingness to help.

Anritsu[®] is a registered trademark of Anritsu Corporation.

Electro-metrics[™] is a trademark of Electro-Metrics, Inc.

EMCO[®] is a registered trademark of EMCO High Voltage Corporation.

FlecTron[®] is a registered trademark of Advanced Performance Materials, Inc.

Hewlett Packard[®] is a registered trademark of the Hewlett Packard Company.

Mini-Circuits[®] is a registered trademark of Scientific Components Corporation.

Narda[®] is a registered trademark of L3 Communications Corporation.

Tektronix[®] is a registered trademark of Tektronix, Inc.

Vitek[®] is a registered trademark of Vitek Systems, Inc.

EXECUTIVE SUMMARY

The **COMbat Wear Integration** (COMWIN) project seeks to develop a man-carried antenna that transmits or receives a signal at any frequency from 2 MHz to 2 GHz while disguising the radio operator's identity. The first goal is to make the antenna compatible with the hand-held radio that will be manufactured in accordance with the Operational Requirements Document of the Joint Tactical Radio (JTR). The second goal is to make it harder for snipers to target the radio operators and disrupt command, control, and communications at the squad level. Integrating the antenna into the uniform of the soldier or marine achieves both goals.

During Fiscal Year 2001 (FY 2001), models of a vest antenna, a helmet antenna, and a whole-body antenna were fabricated and tested. The vest antenna has a voltage standing wave ratio (VSWR) of less than 3:1 over the range 37 to 351 MHz. The helmet antenna has a VSWR of less than 3:1 over the 400- to 1800-MHz frequency range. The whole-body antenna has a VSWR of less than 2:1 over the 5- to 30-MHz frequency range. Thus, if taken together, the three-antenna COMWIN system has a VSWR of less than 3:1 over almost the entire 2-MHz to 2-GHz frequency range. The antenna is still usable at those frequencies at which the VSWR requirement is not met.

During April and May 2001, tests on the vest antenna were conducted at the SPAWAR Systems Center (SSC San Diego) Antenna Range. The gain at boresight varied from around -10 dBi at frequencies less than 100 MHz to 3 dBi at frequencies near 200 and 400 MHz. The polarization was vertical for all frequencies at boresight. The difference between vertical and horizontal polarization is often more than 10 dB. The radiation patterns are isotropic in the horizontal plane for frequencies less than 250 MHz. Near frequencies of 400 MHz, the patterns develop nulls near the positions of the arms. These nulls can be as large as 20 dB. The elevation patterns have only shallow nulls. For the higher frequencies, the maximum in the elevation pattern is often at angles near 90°.

Through the spring of 2001, tests on the helmet antenna were conducted at the SSC San Diego Anechoic Chamber. Similar to the vest antenna, the measurements included gain, azimuth patterns, and elevation patterns. The vertical gain at boresight had significant variations. The minimum was -15 dBi at 400 MHz and the maximum was greater than 0 dBi. Unlike the vest antenna, the helmet antenna had significant horizontal polarization at boresight and nulls in the azimuth pattern at all frequencies. The horizontal polarization was larger than the vertical at 400 MHz and equal to the vertical at frequencies less than 800 MHz. For the higher frequencies, the vertically polarized gain at boresight was almost always larger than the horizontal. The elevation pattern varied significantly at all frequencies.

In February 2001, tests on the whole-body antenna were conducted at the SSC San Diego Model Range in the 2- to 30-MHz frequency range. The gain of the whole-body antenna was compared to the gain of a 35-foot whip antenna. The gain of the whole-body antenna was less than that of the 35-foot whip antenna at all frequencies. Because external noise usually dominates the transmission of signals, high gain is usually not a significant requirement. At frequencies higher than 20 MHz, the gain of the whole-body antenna is about 10 dB less than that for the 35-foot whip antenna. No radiation patterns were obtained.

PRC-148 radios were used to determine the effectiveness of the vest antennas as part of a communications system. The experiments consisted of one radio with the standard antenna transmitting and the other radio with the COMWIN vest antenna receiving. A scale of 0 (unintelligible) to 5 (crystal clear reception without static) quantified the reception of the time. The COMWIN antenna was evaluated as a transmitter and a receiver. Experiments were conducted over

distances from 320 m to 4.7 km and compared to results of the standard antenna in similar arrangements. The power used varied from 0.1 to 5 W. The orientation of the COMWIN antenna was at the four cardinal points (north, east, south, west), either vertical or horizontal. Similarly, the standard antenna for the PRC-148 radio was either vertical or horizontal, pointing north, east, south, or west. The COMWIN antenna was tested in a stationary mode or while the wearer was walking. The primary factor that affected the intelligibility of the signal was the terrain. Hills degrade the signal received by the COMWIN antenna and the standard antenna. The COMWIN antenna can transmit and receive at the frequencies measured: 63.9, 139.3, 226.5, 258.5, 337.5, and 435.1 MHz. In most cases, the COMWIN antenna worked as well as the standard antenna. There was an asymmetry between transmit and receive. Often, the standard antenna could not receive the transmissions from the COMWIN antenna at as far a range as the reverse situation. Research must be done to understand this asymmetry.

The whole-body antenna received the transmissions of station WWV in Boulder, CO. The whole-body antenna received the beeping signal every second, with the announcement of time every minute with a clarity only marginally different from the 35-foot whip antenna. The 35-foot whip antenna is the standard high-frequency (HF) antenna for U.S. Navy ships. The signals received were at frequencies of 5, 10, 15, and 20 MHz.

The helmet antenna received a 2.4-GHz video signal transmitted over a wireless LAN with a data rate of 11 Mbps. The wireless LAN used an 802.11 protocol. The transmitting antenna was a microstrip type. The image of the continuous movement of the second hand of a clock was received for viewing by a second microstrip antenna attached to a laptop computer. When the link margin was strong, the image of the second hand changed at increments of approximately 1 s. When the margin began failing, the second hand varied at increments of 5 s, showing lower data transfer rates. At a distance of 30 m, the microstrip antenna began exhibiting the behavior of changing in increments of 5 s. At a distance of 60 m, the image of the second hand froze and eventually the screen blackened. The output of the helmet antenna was then inserted into the port on the microstrip antenna. The image of the clock immediately began changing nearly continuously. This behavior continued out to a distance of 160 m. At this distance, the image of the second hand changed in increments of 5 s, indicating that the link margin of the helmet antenna was beginning to fail.

The three antennas are now integrated into one system. Although the radio that will provide the signal for the COMWIN antenna does not yet exist (scheduled for FY 2004), it is expected that a control word will emerge from the radio when the operator enters the choice of frequency and waveform. This control word will activate a single-pole, three-throw (SP3T) switch. The switch will then determine which antenna will radiate the signal. In the absence of a radio, a single-pole, four-throw (choice of three antennas and an off switch) worn on the wrist of the radio operator will connect to the radio frequency (RF) SP3T switch. The wrist-borne switch will direct the voltage from three 9-V batteries in series to change the choice of antennas.

The radiation hazards of the vest and helmet antenna were measured using electric field and temperature sensors at the Naval Health Research Center–Detachment at Brooks Air Force Base (AFB) in San Antonio TX. Power levels of 50 W were input into the vest and helmet antennas, which were worn by plastic mannequins filled with jell to simulate a human. The researchers at Brooks AFB have conducted many experiments using these “jell men” in various frequency ranges. An implantable electric field sensor was inserted into the mannequin and readings obtained. The vest was used at frequencies between 30 and 400 MHz. The helmet antenna was used for frequencies between 400 and 1000 MHz. At the 24 locations (3 depths and 8 spots on the back of the vest antenna), there were two locations at which a radiation hazard was found for a scaled input power of

5 W and a frequency of less than 90 MHz. At frequencies above 200 MHz for the vest and the three locations in the helmet, there was little radiation hazard, even for 50-W input power. The radiation hazard of the vest can be solved in a straightforward manner. The exploration of the solution must wait to the beginning of FY 2002.

The FY 2002 program will be first to mitigate the radiation hazard of the vest and then to continue the program of exploring the range of the COMWIN antenna as a function of frequency, input power, terrain, and orientation. COMWIN system investigations will focus on the vest antenna.

CONTENTS

EXECUTIVE SUMMARY	iii
INTRODUCTION	1
SUMMARY OF RESULTS FROM PREVIOUS YEARS	1
GOALS FOR FY 2001	3
VEST ANTENNA	5
IMPEDANCE/VSWR MEASUREMENTS	7
ANTENNA MEASUREMENTS	10
RADIO TESTS	17
HELMET ANTENNA	25
IMPEDANCE/VSWR MEASUREMENTS	26
ANTENNA MEASUREMENTS	27
VIDEO DATA TRANSFER TESTS	35
WHOLE-BODY ANTENNA	39
IMPEDANCE/VSWR MEASUREMENTS	40
ANTENNA MEASUREMENTS	41
RADIO TESTS	42
INTEGRATION OF THREE ANTENNAS INTO ONE SYSTEM	43
RADIATION HAZARD MEASUREMENTS	45
ELECTRIC FIELD MEASUREMENTS IN EMPTY VEST ANTENNA.....	45
MEASUREMENTS OF ELECTRIC FIELDS WITHIN THE BODY.....	47
CONCLUSIONS	69
REFERENCES	71

Figures

1. Mark IIIA vest antenna.....	5
2. Mark IIIB vest antenna (front)	6
3. Feed at rear of Mark IIIB vest antenna	7
4. VSWR versus frequency in 30- to 100-MHz range for Mark IIIA vest antenna with and without suspenders.....	8
5. VSWR versus frequency in 100- to 500-MHz range for Mark IIIA vest antenna with and without suspenders.....	8
6. VSWR versus frequency in 30- to 500-MHz range for Mark IIIA vest antenna with and without suspenders.....	9
7. Comparison of VSWR versus frequency of Mark IIIA (with switch) and Mark IIIB (without switch).....	10
8. Gain of Mark IIIA vest antenna at boresight versus frequency	11
9. Azimuth radiation patterns of Mark IIIA vest antenna.....	13
10. Elevation patterns for Mark IIIA vest antenna for azimuth angle 0°	15
11. Topographic map of Point Loma showing measurement sites	18
12. Mark III helmet antenna (front)	25
13. Mark III helmet antenna (rear)	26
14. VSWR versus frequency of Mark III helmet antenna worn by a person	27
15. Gain of Mark III helmet antenna in vertical and horizontal polarizations.....	28
16. Azimuth radiation patterns for Mark III helmet antenna at frequencies of 500 to 1800 MHz in steps of 100 MHz.....	28
17. Elevation radiation patterns for Mark III helmet antenna at frequencies of 500 to 1800 MHz in steps of 100 MHz for an azimuth angle of 0°	31
18. Elevation radiation patterns at frequencies of 500 to 1800 MHz in steps of 100 MHz for azimuth angle of 90°	33
19. Helmet antenna transferring video data.....	36
20. Whole-Body antenna (front view).....	39
21. Whole-Body antenna (rear view)	40
22. VSWR versus frequency for whole-body antenna.....	41
23. Gain of whole-body antenna compared to 35-foot whip antenna	42
24. Narda® SEM133 SP3T switch to be used to channel signal from JTR to appropriate antenna in COMWIN system	44
25. VSWR versus frequency of COMWIN antenna for three different modes of SP3T switch...	44
26. EMCO® isotropic E-field sensor used for RADHAZ studies.....	46
27. Electric fields within empty COMWIN vest antenna versus location and frequency	47
28. Implantable E-field probe from SARTest LTD	48
29. Probe with cover assembled (left) and with cover removed (right).....	49
30. Mannequin filled with jell.....	50
31. Comparison of VSWR versus frequency of vest antenna on mannequin and on various researchers in 30- to 100-MHz range	51
32. Comparison of VSWR versus frequency of vest antenna when worn by mannequin and by person in 100- to 500-MHz range.....	51
33. Specific absorption rate in W/kg for vest antenna versus frequency for three different compositions of jell and three different depths of probe for Site M.....	62
34. Specific absorption rate in W/kg for vest antenna versus frequency for three different compositions of jell and three different depths of probe for Site N	63
35. Experimental arrangement for measurement of electric fields within helmet antenna	64
36. VSWR versus frequency of helmet antenna on a mannequin and on a person.....	65

Tables

1. Quality of reception by COMWIN antenna from transmissions using PRC-148 radio using standard antennas with vertical polarization	19
2. Record of transmissions between DVM at the lighthouse at Cabrillo Point and RCA walking along Woodward Road	20
3. Record of transmissions between RCA using COMWIN vest antenna and DVM using standard antenna for PRC-148 radio	22
4. Quality of reception of a signal of a particular frequency and polarization	24
5. Composition by weight of jell man for various frequency ranges	52
6. Electric field data for 41-MHz composition and depth of probe 1 cm into back of mannequin	53
7. Electric field data for 41-MHz composition and depth of probe near center of mannequin ..	54
8. Electric field data for 41-MHz composition and depth of probe near front of mannequin	55
9. Electric field data for 200-MHz composition and depth of probe 1 cm into back of mannequin	56
10. Electric field data for 200-MHz composition and depth of probe at center of mannequin	57
11. Electric field data for 200-MHz composition and depth of probe 1 cm into front of mannequin	58
12. Electric field data for 300-MHz composition and depth of probe 1 cm into back of mannequin	59
13. Electric field data for 300-MHz composition and depth of probe at center of mannequin	60
14. Electric field data for 300-MHz composition and depth of probe 1 cm into front of mannequin	61
15. Electric fields measured with jell man when 50 W of power are input to helmet antenna	66

INTRODUCTION

The **COMbat Wear INtegration** (COMWIN) antenna project seeks to develop a man-carried antenna that meets two goals. The first goal is to transmit or receive a signal at any frequency between 2 MHz and 2 GHz. This goal is based upon the Operational Requirements Document (ORD) of the Joint Tactical Radio System (JTRS) published in March 1998 (ORD for JTR, 1998). The second goal is to visually hide the radio operator's identity. This goal is based upon reports from the Vietnam War and the Russian misadventure in Chechnya that snipers preferentially target radio operators and the officers nearby (Thomas, 1999). The snipers seek to disrupt the command, communications, and control functions at the squad level. Making the radio operator indistinguishable from other soldiers would help protect the squad from disruption. Snipers can often easily identify the radio operator by sighting the large whip antenna attached to a box on the soldier's back.

Integration of the antenna into the uniform of the soldier can help meet both aims. The method used by this project has the acronym **COMbat Wear INtegration** (COMWIN). This acronym also refers to the project and the system. Integration of the antenna into the uniform provides hides the identity of the radio operator. The radio operator would be indistinguishable from any other soldier. The integration also provides the maximum amount of surface area for a given length. Increasing the surface, if done cleverly, can increase the bandwidth of an antenna by increasing the number of paths that a signal can use to radiate energy.

SUMMARY OF RESULTS FROM PREVIOUS YEARS

The COMWIN project began in May 1999. Literature research was conducted and preliminary models were developed using the GNEC software under the leadership of Professor Jovan Lebaric and Professor Richard Adler of the Naval Postgraduate School (NPS). The GNEC software program uses method of moments to predict impedance and radiation patterns. Professor Lebaric and his colleagues decided that no one antenna could possibly cover the 2-MHz to 2-GHz frequency range. Lebaric suggested three antennas. A vest antenna would cover the 30- to 500-MHz range. A helmet antenna would cover the 500- to 2000-MHz range. Finally, a whole-body antenna would cover the HF range, 2 to 30 MHz. The COMWIN project developed from Lebaric's original concept.

Lebaric proposed a brilliant way to increase antenna bandwidth. In the vest antenna, there is a gap (width, approximately 1 inch) that separates the device into an upper and lower part. The feed is located at the rear of the vest. The vest acts like a fat dipole antenna. The impedance becomes largely capacitive at the higher frequencies. Lebaric put a shorting strap at the front of the vest. This addition provided inductance that largely cancelled the capacitance so that the impedance became resistive. Another way to look at this addition is to think of the vest as the combination of a dipole antenna and a loop antenna. These antennas have maximums and minimums of the voltage standing wave ratio (VSWR) that vary periodically with frequency. The minimums of the VSWR for the dipole antenna and loop antenna alternate. Combining the two antennas provides impedance that varies much less than either antenna would provide separately. A prototype of the vest antenna was fabricated at the SSC San Diego Model Shop in August 1999 and tested on the SSC San Diego Model Range.

The results confirmed the predictions qualitatively and quantitatively. The measured impedance was usually within 10% of the predicted impedance. The theoretical and experimental azimuth and elevation patterns were similar. The VSWR was less than 3:1 over the 100- to 500-MHz frequency range. The VSWR was very high for the lower frequencies. In the upper frequencies, the gain varied between 2 and 6 dBi. In the frequencies less than 200 MHz, the azimuth pattern was nearly omni-

directional. For the higher frequencies (later determined to be 250 MHz), the patterns had nulls. Nulls at frequencies higher than 250 MHz have continued for all subsequent models (Adams et al., 1999).

For FY 2000, Lebaric designed a helmet antenna that had many of the same features as the vest (gap parallel to the ground and shorting strap on the side opposite to the feed). Lebaric gave this helmet antenna to SSC San Diego for further testing. Lebaric also suggested that enlarging the path taken by the wave would allow better matching of the vest antenna at frequencies less than 100 MHz. Making the gap into a saw-tooth pattern would accomplish this lengthening of the path. The result for the vest was that the VSWR for the lower frequencies improved, but at the cost of increasing the VSWR in the higher frequencies. Vest antenna gain was measured at all frequencies between 50 and 400 MHz. Although for some frequencies below 100 MHz the gain was less than -10 dBi, the gain was almost always larger than 0 dBi for frequencies greater than 100 MHz (Adams et al., 2000).

As an alternative to the helmet antenna fabricated at NPS, SSC San Diego fabricated one that had a saw-tooth pattern. The VSWR of the SSC San Diego helmet antenna was excellent, less than 3:1 for almost all frequencies between 500 and 2000 MHz. The gain of the SSC San Diego helmet antenna, however, was much less than that for NPS. The difference was often as much as 10 dB. The SSC San Diego helmet antenna also had a much wider gap than the NPS helmet antenna (Adams et al., 2000).

Radiation hazard (RADHAZ) studies began. The matching circuit from the vest antenna model from FY 1999 was changed to accommodate more power (the RF transformer used for matching had a maximum power rating of 0.25 W). Studies were also conducted to demonstrate that the electric field within the vest was proportional to the square root of the input power. Such a demonstration of scaling was important because of the limitation on power caused by the RF transformer still on the FY 2000 model. Extrapolation from low-power measurements would be one method to demonstrate the safety of the antenna from radiation hazards.

Measurements of the electric field within the FY 1999 and FY 2000 vest antennas indicate that the saw-tooth pattern of the gap allowed more fields to leak into the body than a straight gap. The extrapolated fields were almost always less for the straight-gap vest antenna. For frequencies around 90 MHz (the FM broadcast band), the electric fields within both models of vest near the feed were higher than those allowed by the Institute for Electrical and Electronic Engineers (IEEE) standards for whole-body exposure. These fields always decreased with increasing distance from the feed. For the saw-tooth patterned vest antenna, the electric field near the feed at frequencies around 300 MHz was larger than that prescribed by the standard.

The matching circuit of the FY 1999 model of vest antenna was changed to allow high levels of input power and to test for heating within the body. As a test, a plastic container of 34 kg of salt water was used. The VSWR of the vest antenna was excellent at frequencies between 250 and 350 MHz. After the input of 50 W of power for 30 minutes, the measured temperature at the end of the experiment was no higher within the 0.1°C resolution of the thermometer than that at the beginning (Adams et al., 2000).

A jell that simulated the dielectric and conductive properties of a person in the 100- to 500-MHz frequency range was mixed. Chou et al. (1984) provided the recipe for the mixture. Measurements of the impedance of the vest on a person or a 34-kg container filled with jell showed the similarity of the mixture to a human. Experiments on measuring the temperature after the input of 50 W of power for 30 minutes showed no heating by the vest antenna. The experiments were repeated five times with similar results. The frequencies used were 250, 300, and 350 MHz (Adams et al., 2000).

GOALS FOR FY 2001

The first goal for FY 2001 was to fabricate and test three antennas that would meet one of the important objectives, a VSWR less than 3:1 over the usable frequency range. This test included a vest antenna (30 to 500 MHz), a helmet antenna (500 to 2000 MHz), and a whole-body antenna (2 to 30 MHz). Not all frequency ranges were equally important. The testing included VSWR versus frequency, gain, and patterns. Any antenna in the HF range was difficult to test on an available facility. Patterns were assumed to be isotropic for the whole-body antenna. The matching circuits for the vest and helmet antennas had to withstand power as large as 50 W so that they could be used in realistic environments.

A second goal was to begin the operational testing of the antennas. This testing included determining the quality of reception by the use of radios that mimicked the action of the ones for the JTRS. There had to be some compromise because of the availability of radios in terms of frequency range. Although gain was one measure of the quality of an antenna, the use of intelligibility of a signal received from one radio to another was an important figure of merit.

The third goal was to perform extensive measurements and analysis of the radiation hazard, especially for the vest and helmet antennas. One aspect that could not be investigated during FY 2000 was the electric field distribution within a realistic body. The investigation during FY 2001 involved using an implanted sensor and jell that contained aluminum powder, a hazardous material because of its flammability. The impedance of the vest antenna over the human body was much different from an empty one. There was no substitute for having experience in measuring these fields in realistic environments.

The final goal was to design a preliminary version of a distribution network. There was one output from the radio. This output had to go to one of three antennas based upon frequency. One method used an impedance matching device that did this selection automatically. Another method used a control signal from the hand-held radio. This latter method needed an electronically controlled switch, which probably implied far greater isolation between inputs to the various antennas. The great isolation that the switches attained made this method the preferred one.

VEST ANTENNA

Based upon the experiences of FY 1999 and FY 2000, the SSC San Diego Model Shop constructed a new model of the vest antenna, the Mark III. The feed was located at the rear. The gap was horizontal. Maximum symmetry was imposed upon the design, symmetry from right to left and top to bottom. Because a human body is wider than it is deep, the symmetry was not complete. Symmetry was broken, as necessary, to improve the VSWR versus frequency measurement. A second reason for using a straight gap (versus the saw-tooth) was a radiation hazard issue. More energy leaked into the body from the saw-tooth gap than from the straight gap.

The most important aspect of the Mark III was that its design considered the effect of the human being wearing the device. Because a human being has a significant impact upon impedance and VSWR, this must be considered. A person in the vest makes matching the antenna easier than it would be for an empty vest.

Figure 1 shows the Mark IIIA vest antenna with the maximum right-to-left symmetry. The height of each panel is the maximum that could fit under the arms. The arms necessarily break the symmetry. Measurements of the VSWR versus frequency indicated that if an additional path could be made to allow the signal to get from front to back, the matching would improve. Suspenders shown in figure 1 provided this additional path. The VSWR for the 30- to 88-MHz frequency range was much lower with suspenders than without. The suspenders had little effect on the impedance in the 100- to 500-MHz frequency range.



Figure 1. Mark IIIA vest antenna.

The Mark IIIA vest antenna had a switch. The switch allowed better matching by breaking up the 30- to 500-MHz frequency range into two smaller ones. Each range could then be matched more optimally. Unfortunately, using a switch for this purpose complicated the distribution network described later in this report. The Mark IIIB antenna omits the switch and uses a value of capacitance between the two frequencies used for the smaller ranges. The Mark IIIB also used snaps to allow easy removal of the vest. Previously, the vest was solid, which required pulling the garment over the wearer's head.

Figure 2 shows the front of the Mark IIIB vest antenna with the shorting strap, snaps, and suspenders.



Figure 2. Mark IIIB vest antenna (front).

Figure 3 shows the feed region of the Mark IIIB vest antenna. A capacitor (56 pF) was inserted in series between the top and bottom portions of the vest. In the Mark IIIA version, a switch caused the signal to go through either a 68-pF capacitor (for the 30- to 100-MHz range) or a 24-pF capacitor (for the 100- to 500-MHz range).



Figure 3. Feed at rear of Mark IIIB vest antenna.

As in all previous models, FlecTron[®], manufactured by Advanced Performance Materials of St. Louis, was used as the conductive material for the antenna. The resistivity of the material was quoted as less than 0.1 ohms per square (Adams et al., 1999). The material is light and flexible. Normal soldering could not be done because of the low melting point of the material. Copper tape was sewn at the locations that required soldering. Cotton material was used as the backing for the antenna to provide shape.

IMPEDANCE/VSWR MEASUREMENTS

An Anritsu[®] 113B Sitemaster was used to measure the VSWR and determine the impedance. This device is a one-port, battery-operated device that measures VSWR at up to 517 frequencies between 5 and 1200 MHz. Weighing only 4 pounds, this device is often taken on ships to diagnose faults and to determine the effect of location on the matching of an antenna. The phase of the reflection coefficient is provided as well as the VSWR. Thus, by some simple calculations, the real and imaginary parts of the impedance can also be determined. The real and imaginary parts were needed for plotting a Smith Chart and determining the value of the capacitance required for optimal matching. In two cases, we compared the results of the Sitemaster to those of an HP 8510C network analyzer. The results for impedance were virtually identical.

Figure 4 presents the VSWR versus frequency of the Mark IIIA vest antenna in the 30- to 100-MHz frequency range. The VSWR for the vest antenna having suspenders was compared with the VSWR of the vest antenna without the suspenders. In the 30- to 100-MHz band, the comparison was especially stark. The percentage of data points for which the VSWR was less than 3 increased from 41 to 89%. The VSWR decreased below 3 as the frequency increased to 37 MHz and remained less than 3. Figure 5 shows a similar plot in the 100- to 500-MHz band. Suspenders had little effect, especially for frequencies higher than 250 MHz. The percentage of data points for which the VSWR

was less than 3 increased from 55 to 63% when suspenders were added. Figure 6 shows the comparison for the 30- to 500-MHz range. The percentage of data points for which the VSWR was less than 3 increased from 48 to 75%. The VSWR was less than 3 for all frequencies between 37 and 351 MHz. The VSWR did not go above 4.5 for all frequencies less than 500 MHz. The discontinuity in the VSWR data in figure 6 was due to the use of the switch and two different values of the capacitor.

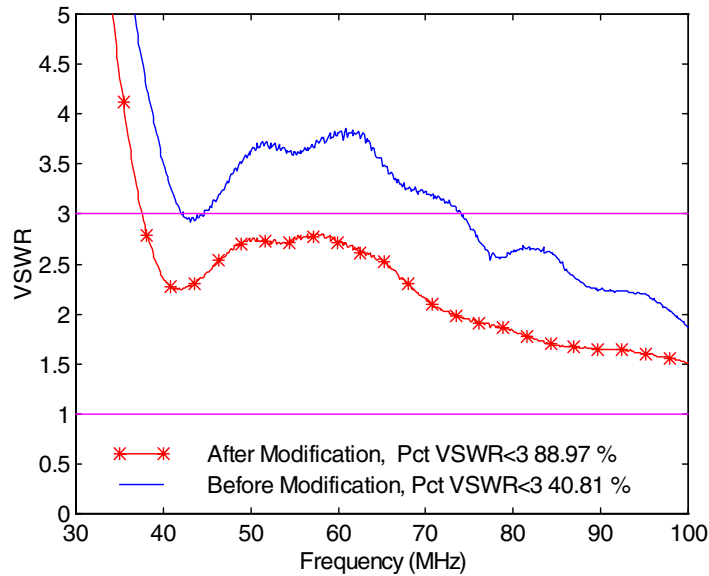


Figure 4. VSWR versus frequency in 30- to 100-MHz range for Mark IIIA vest antenna with and without suspenders.

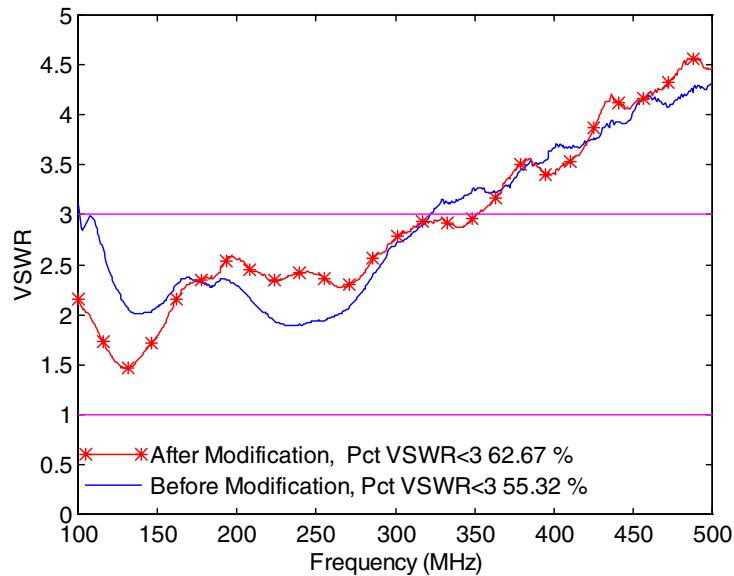


Figure 5. VSWR versus frequency in 100- to 500-MHz range for Mark IIIA vest antenna with and without suspenders.

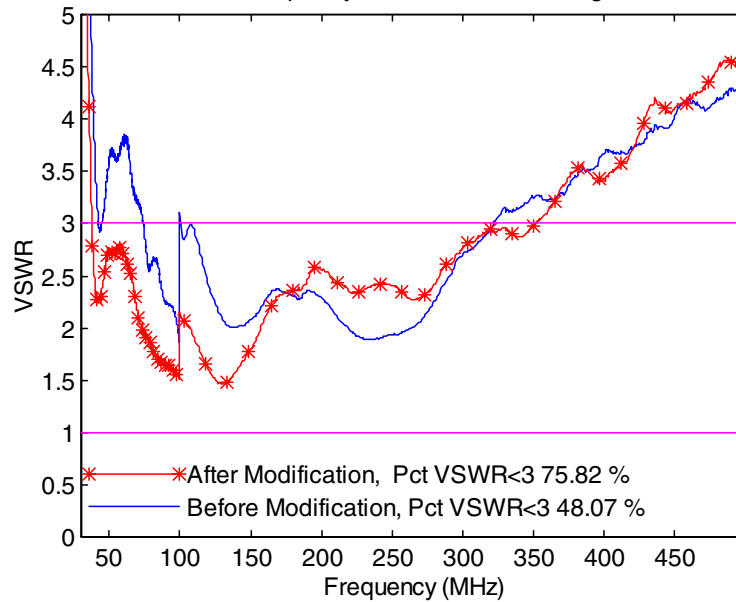


Figure 6. VSWR versus frequency in 30- to 500-MHz range for Mark IIIA vest antenna with and without suspenders.

As figure 6 shows, suspenders improve the VSWR versus frequency at most of the frequencies between 30 and 100 MHz and some of those between 100 and 500 MHz.

Omitting the switch and using a capacitor with a value between the two frequencies used in the Mark IIIA represents a compromise. The compromise is necessary for the implementation of the COMWIN system.

Figure 7 compares the VSWR for the Mark IIIA (with switch) to that of the Mark IIIB (without switch). In the Mark IIIB, a value of 56 pF was used for the matching circuit. Figure 7 shows that the compromise is very effective.

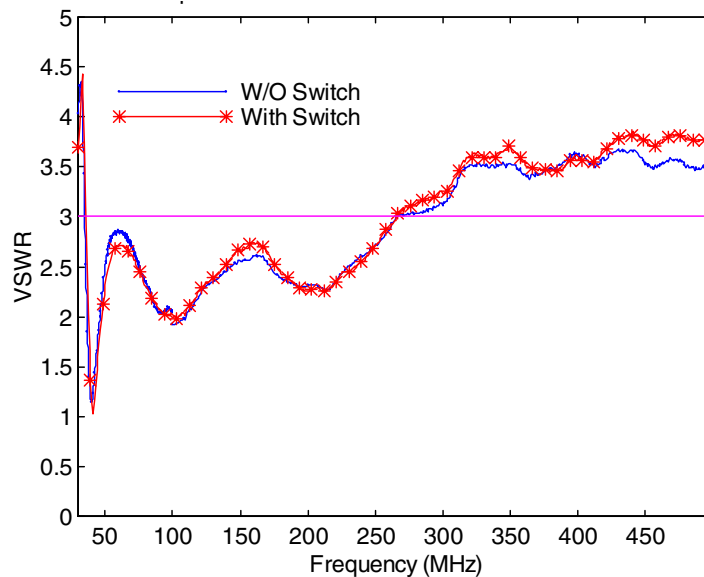


Figure 7. Comparison of VSWR versus frequency of Mark IIIA (with switch) and Mark IIIB (without switch).

ANTENNA MEASUREMENTS

In April, May, and June 2001, measurements of the parameters of the Mark IIIA vest antenna were obtained. The measurements included gain at boresight (vertical and horizontal polarization), azimuth patterns, and elevation patterns. Each parameter is important in assessing the figure of merit of an antenna. Gain is the parameter that determines the range at which the signal can be attained for a given wavelength, power, and sensitivity. The azimuth patterns determine the ability to communicate in all directions without knowledge of the location of the receiver. The elevation pattern is important because radio operators must communicate with aircraft and helicopters.

The measurement site was the SSC San Diego Antenna Range (Buildings 584 and 592). The transmitter site was a shed located on the south side of Woodward Road. The receiver site was the West Tower located on the north side of Woodward Road, 270 m feet away from the transmitter. Woodward Road is located in a 90-m deep valley that leads to the Pacific Ocean. No land or structure reflects signals directed toward the West Tower (next stop, Alaska). The steep slope of the valley attenuates reflections from the ground. The height of the tower is approximately 15 m.

The transmitter was composed of a Hewlett Packard® 83712B synthesized continuous wave (CW) signal generator that input a signal to a 550L E-Systems 50-dB amplifier. The frequency range of the amplifier was 1 to 400 MHz. Beyond a frequency of 410 MHz, the gain of the amplifier dropped rapidly. The 1-dB compression point of the amplifier was 47 dBm. A Narda® 3020A bi-directional coupler (25-dB nominal attenuation) attached to Hewlett Packard® 6428A and 436A power meters measured the power input to the transmitting antenna. For frequencies below 90 MHz, the transmitting antenna was usually a Single-Channel Ground and Airborne Radio System (SINCGARS) antenna designed to be operated on a jeep. For the higher frequencies, a log periodic antenna was used.

On the West Tower, there is a turntable that nominally has three axes of motion. Only one axis can be used at a time. Elevation patterns were limited when one of the turntable's azimuth axes malfunctioned. The sensor used was a calibrated Tektronix® 495 P spectrum analyzer. Using such a narrow-band sensor made identifying the transmitter signal easy, even with nearby noise. Only in the frequency modulation (FM) broadcast band was such rejection impossible. A calibrated Electrometrics™ biconical antenna was used as the standard for measurement of the antenna gain. An attachment ("bunny ears") was put onto the standard gain antenna to measure signals in the 30- to 90-MHz range.

Figure 8 presents the gain at boresight of the Mark IIIA vest antenna versus frequency between 30 and 400 MHz for vertical and horizontal polarization. These measurements were made on 12 through 19 April 2001. The vest antenna was on a Styrofoam figure. The matching of the antenna had been optimized for a person. The mismatch had a significant impact upon the gain and efficiency. These measurements will be repeated during FY 2002 with a person wearing the antenna to determine the effect.

The average of the gain for frequencies less than 100 MHz was -10 dBi. The gain increased to 3 dBi and 0 dBi at 200 and 400 MHz, respectively. There was a dip in the gain down to -10 dBi at frequencies around 270 MHz. The average gain for vertically polarized signals in the 30- to 85-MHz range was -9.1 dBi. For frequencies between 110 and 450 MHz, this average was -3.0 dBi. For horizontally polarized signals, this average decreased to -13.3 dBi (30 to 85 MHz) and -15.3 dBi (110 to 450 MHz). The horizontal gain was important because the soldier must communicate with a vertically polarized antenna, even when prone. The vest antenna provided many paths for the signal to emerge with horizontal polarization.

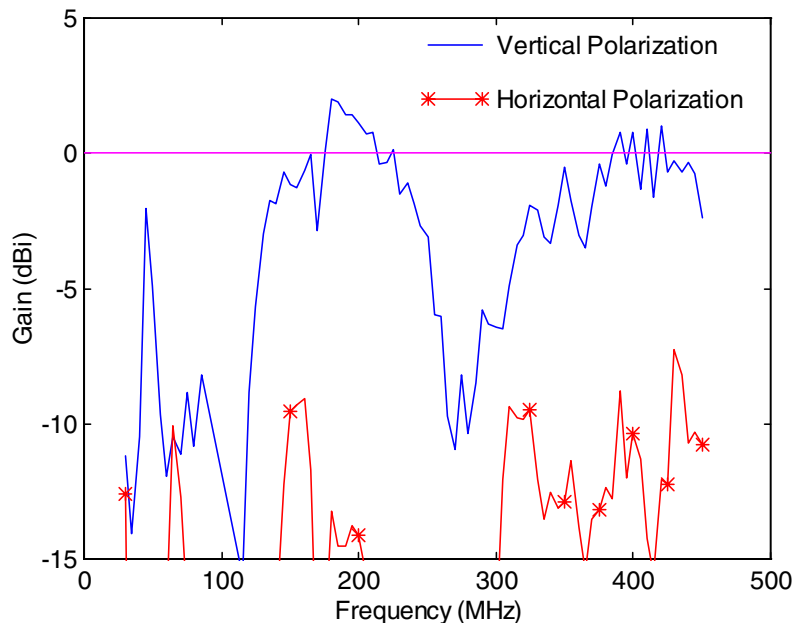


Figure 8. Gain of Mark IIIA vest antenna at boresight versus frequency.

Azimuth patterns were obtained on 23 May 2001 by writing down the value of the signal on the spectrum analyzer when the turntable showed an angle divisible by 5. The speed of the turntable was very low. The frequencies at which the measurements were obtained were 50, 125, 150, 170, 200, 225, 250, 275, 300, 350, and 400 MHz. Large values of the noise at 175 MHz prevented exact 25-MHz increments.

Figure 9 presents the azimuth patterns in the horizontal plane for the Mark IIIA vest antenna. The patterns were normalized to the value at boresight. Because figure 8 presented the data for the gain at boresight compared to an isotropic source, the conversion to gain as a function of angle was straightforward. The pattern at 50 MHz showed distortion from a purely isotropic one. For frequencies between 125 and 225 MHz, the pattern was almost perfectly isotropic. As the frequency increased, two nulls developed. The location of the nulls migrated from near the feed (at 300 MHz) to near the arms (at 400 MHz). Nulls in the pattern for frequencies greater than 250 MHz have occurred for every model of the vest antenna. The antenna becomes electrically large for such frequencies. Without significant research into a radical new design, this will be a feature present in all models.

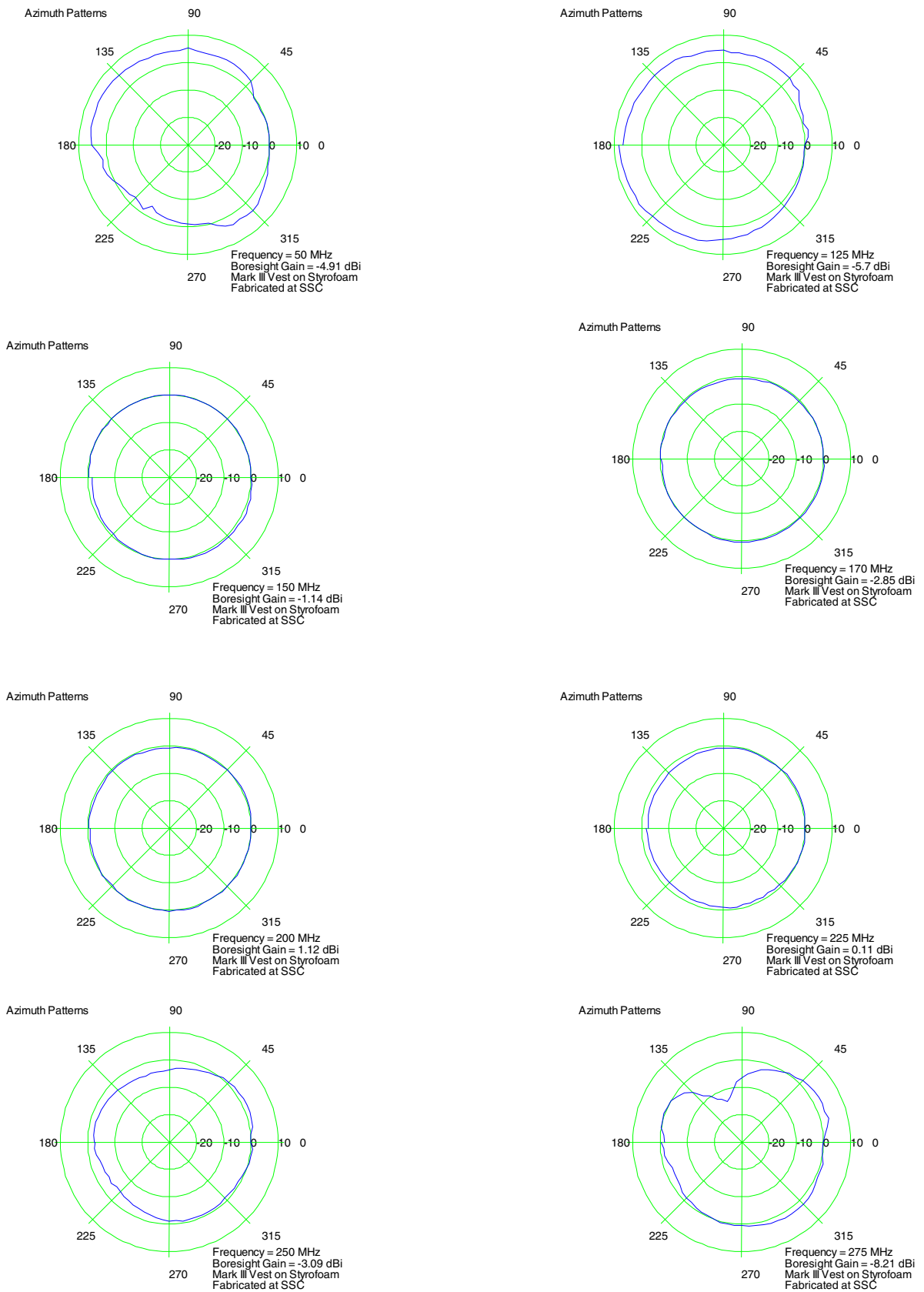


Figure 9. Azimuth radiation patterns of Mark IIIA vest antenna.

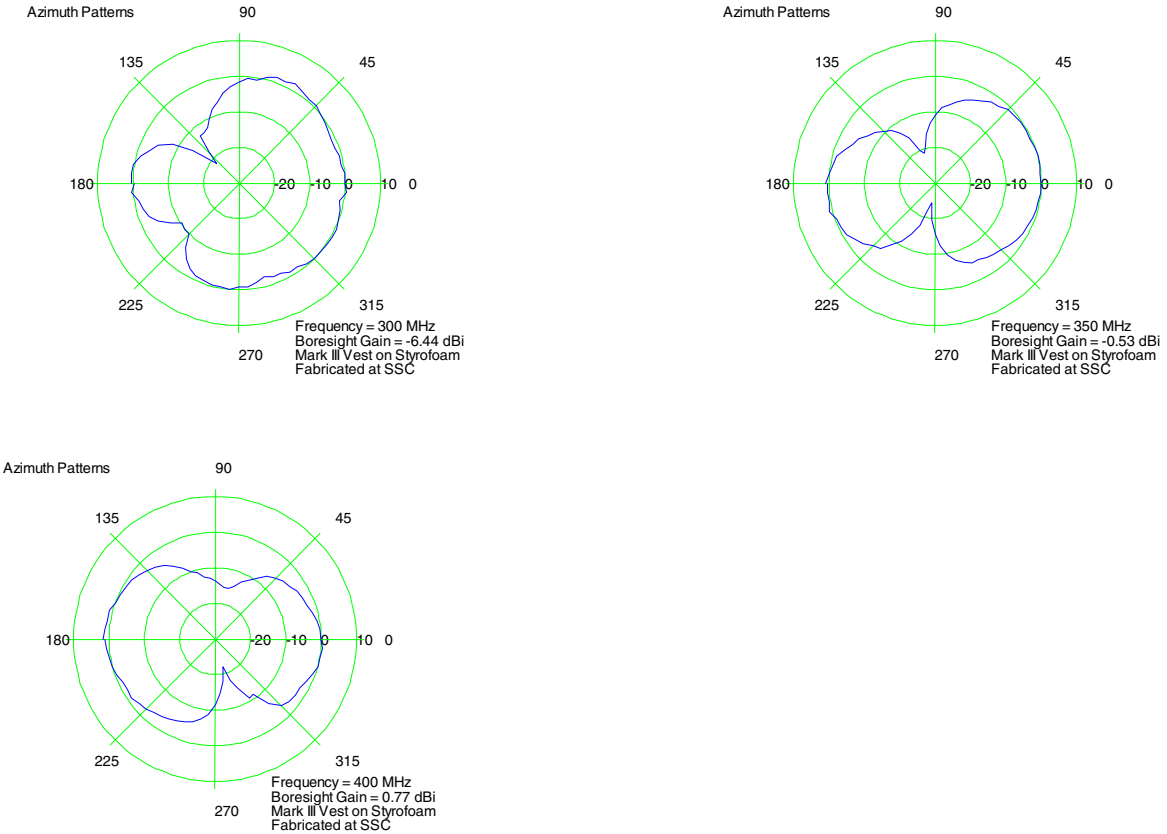


Figure 9. Azimuth radiation patterns of Mark IIIA vest antenna (continued).

Elevation patterns were obtained on 24 and 25 May, and 14 June 2001, in a method similar to the azimuth patterns. A malfunction of one of the axes of the turntable hindered the measurement of the elevation pattern at azimuth angles other than 0°. Figure 10 shows the elevation patterns of the Mark IIIA vest antenna for the same set of frequencies as the azimuth. As in the azimuth patterns, the signal level has been normalized to that measured at boresight. One interesting feature was that at the higher frequencies, the maximum of the elevation pattern occurred at the higher elevation angles. Thus, at frequencies such as 225 to 400 MHz, the soldier could communicate easily with aircraft.

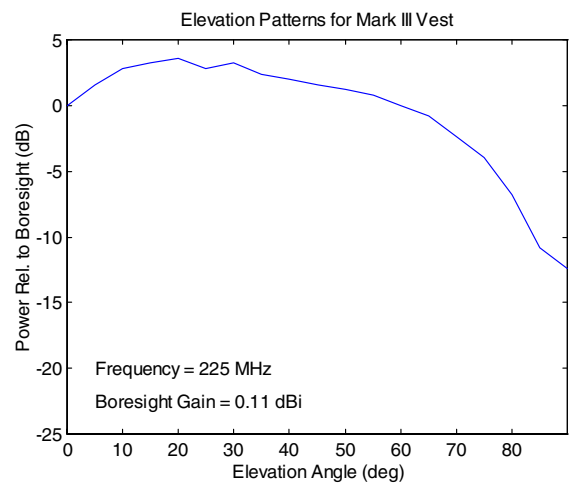
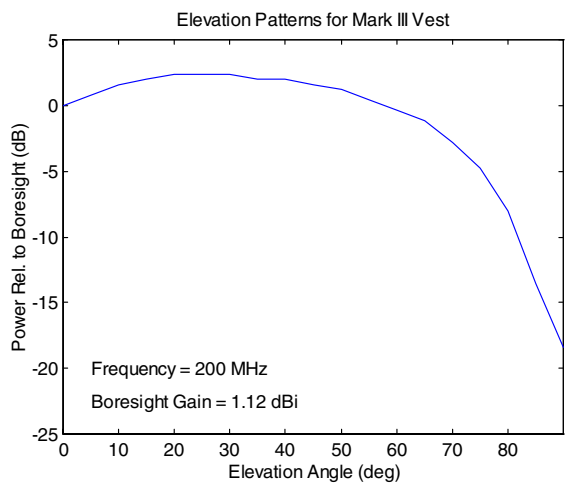
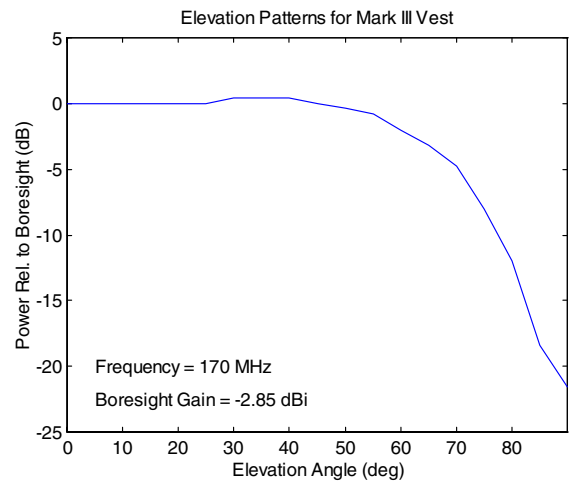
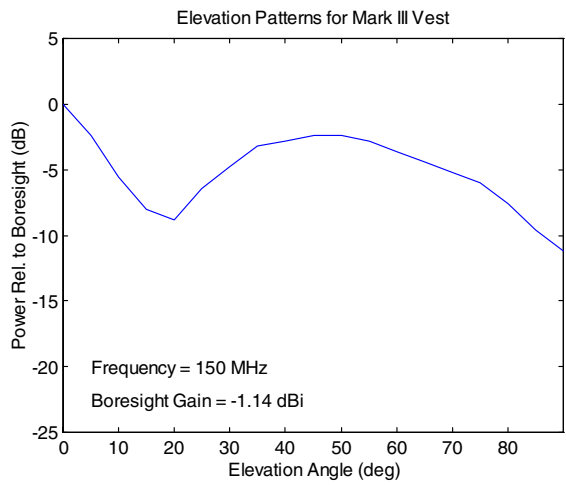
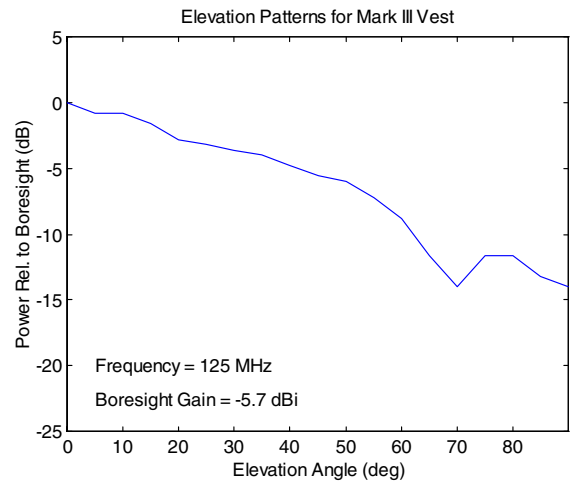
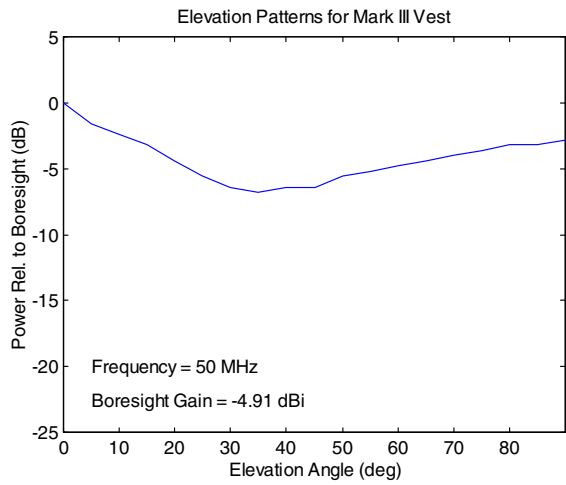


Figure 10. Elevation patterns for Mark IIIA vest antenna for azimuth angle 0°.

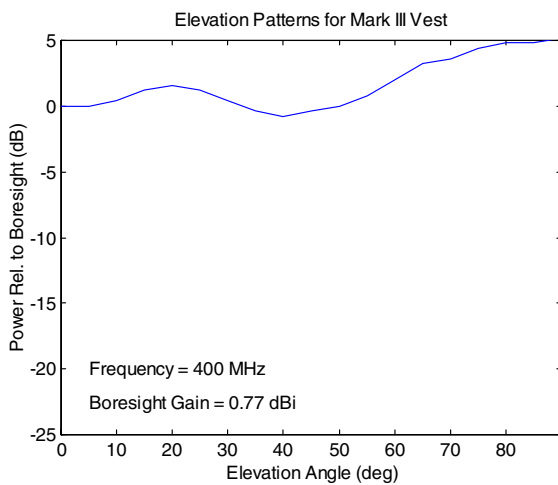
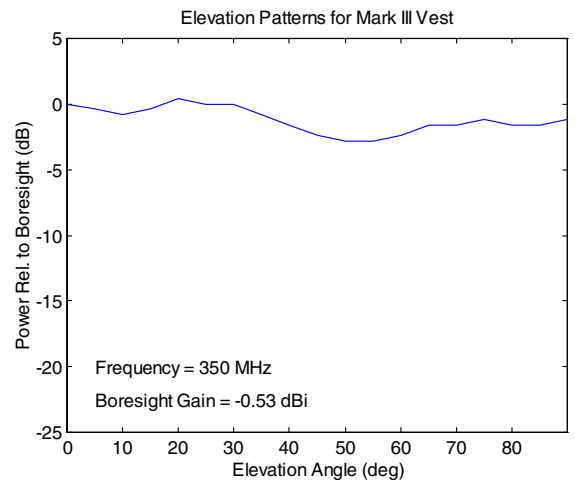
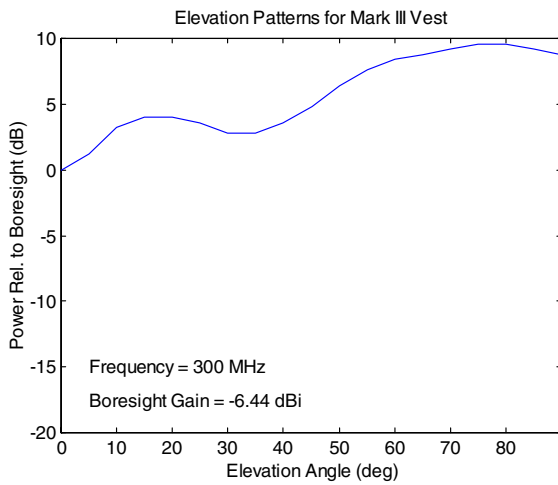
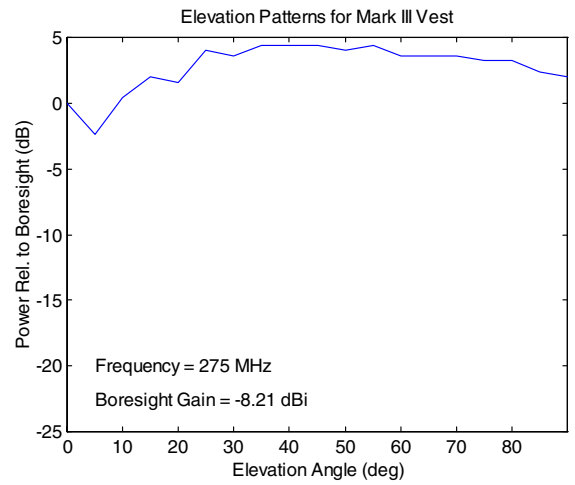
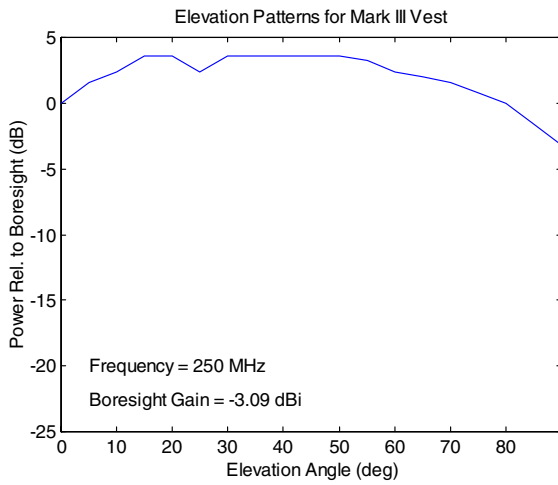


Figure 10. Elevation patterns for Mark IIIA Vest Antenna for azimuth angle 0°. (continued)

The presence of nulls is one of the detracting features of the vest antenna in the COMWIN system. The dimensions are determined by a person's size. Without significant research into dividing the antenna into small elements that can be combined with phase shifts and amplitude redistribution, this feature will probably remain unchanged. Even if some scheme were developed to use phased-array techniques, changes in posture and normal wear and tear would probably prevent successful field implementation. Such a development would also greatly increase weight.

RADIO TESTS

An important aspect of the FY 2001 testing program was the use of the antenna with radios. Two PRC-148 radios (manufactured by THALES Communications Inc.) provided the voice signal received by the vest antenna. The PRC-148 radios transmitted or received a signal with frequencies between 30 and 512 MHz at power levels of 0.1, 0.5, 1, 3, and 5 W. Up to 99 frequencies could be programmed into the radios. Two antennas were included with each radio. The first antenna was a 1.3-m long-whip antenna designed for the 30- to 88-MHz range. The nominal gain for this antenna was -10 dBi. The second antenna was a short-whip antenna that operated at frequencies higher than 100 MHz. The gain of the short-whip antenna was nominally -10 dBi.

The Frequency Coordinator in the San Diego area assigned us a series of six frequencies. These frequencies were 63.9, 139.275, 226.5, 258.5, 337.5, and 435.075MHz. At distances of 320 m, we used only the lowest power. At distances of 4.7 km, we used the highest power. A series of experiments was conducted to determine if the vest antenna could transmit or receive an intelligible signal while the wearer was walking. The test was successful. As a comparison, the standard antennas were tested under similar conditions. If the results for the vest antenna and the long-whip antenna had been identical, the COMWIN system would still be the preferable system because the COMWIN system integrates with the uniform, provides broadband character, and disguises the identity of the radio operator.

Four distinct types of experiments were conducted. In the first experiment, one person (Daryl Von Mueller [DVM]) with a PRC-148 radio with a standard antenna was stationed near the lighthouse and Coast Guard Station at the end of Point Loma. A second person (Richard C. Adams [RCA]) wearing the Mark IIIA vest antenna was located on the top of Building 323, located on Woodward Road adjacent to the Pacific Ocean. Building 323 was chosen because we could see the lighthouse with binoculars. Intelligibility as a function of power level, frequency, and orientation of the wearer (vertical or prone facing the four cardinal points) was determined. In the second experiment, DVM was at the lighthouse and RCA started from Building 323 and walked north along Woodward Road. DVM transmitted the time every minute. RCA responded 30 seconds later. The minimum and maximum distances were 3.3 and 4.7 km, respectively (a fence blocked the end of the road). Large hills also blocked the signal at many locations. A third experiment was similar to the second in that RCA walked north on Woodward Road. The primary difference was that DVM was located at the Joint Tactical Information Distribution System (JTIDS) tower at a height above sea level of 130 m. The line-of-sight distance was much less than the second experiment. A fourth experiment centered on short-range communication (distance of 320 m). DVM was located in the parking lot of the SSC San Diego Model Range. RCA was located at the West Tower. RCA remained vertical, but faced the four cardinal points. DVM changed the orientation of the whip antenna attached to the PRC-148 radio from vertical to horizontal. He also pointed the antenna to the four cardinal directions. Changing the orientation of a transmitting whip antenna is not the same as changing the orientation of the receiving antenna. The propagation characteristics depend on the polarization of the wave.

Figure 11 is a map of the Point Loma area and the geographical coordinates (determined by a hand-held GPS receiver) of the measurement sites. Few locations in the Point Loma region have unobstructed views of more than 5 km. The SSC San Diego Model Range is on a mesa overlooking the Pacific Ocean. Woodward Road is a winding one that goes behind several hills.

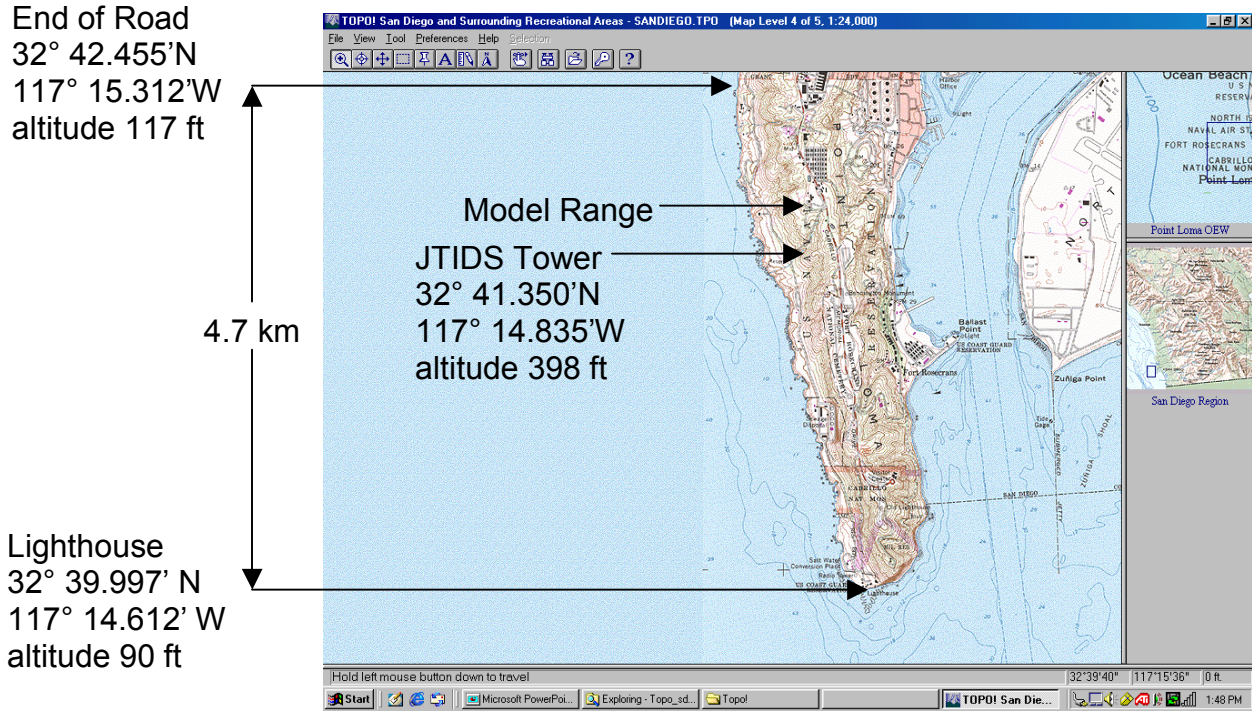


Figure 11. Topographic map of Point Loma showing measurement sites.

As a first test, we sought to determine how well the antenna worked while the wearer was vertical compared to horizontal. DVM, with the standard antenna, transmitted at a frequency of 63.9 MHz at an input power of 0.5 W. The transmission heard by RCA using the COMWIN antenna was clear. RCA then lay down so that the COMWIN antenna was horizontal. The transmission became unintelligible. When the input power to the transmitting radio was increased to 1 W, the transmission became intelligible again, although with some static. The clarity depended significantly upon the direction the COMWIN antenna was facing. The worst reception occurred when the bottom of the COMWIN antenna faced the transmitter. The best reception occurred if the COMWIN antenna was oriented perpendicular to the transmitter. Further experiments are described below.

Table 1 summarizes Experiment 1 results. The transmitter and receiver were stationary. DVM was located at the lighthouse near $32^{\circ} 39.997' N$ latitude, $117^{\circ} 14.612' W$ longitude. RCA was located on the roof of Building 323 near $32^{\circ} 41.798' N$ latitude, $117^{\circ} 15.205' W$ longitude. The distance between these two sites was 3.46 km. If RCA was facing south, he was directly facing DVM. DVM remained vertical on all occasions and used the long-whip antenna for transmitting at 63.9 MHz and the short-whip antenna for transmitting at other frequencies.

Table 1. Quality of reception by COMWIN antenna from transmissions using PRC-148 radio using standard antennas with vertical polarization.

Rx Polarization	Rx Direction	Tx Power (W)	63.9 MHz	139.275 MHz	226.5 MHz	258.5 MHz	337.5 MHz	435.075 MHz
Vertical	West	5	5	5	3	3	3	3
Vertical	South	5	5	5	3	3	2	3
Vertical	East	5	5	5	3	3	2	3
Vertical	North	5	5	5	3	3	2	3
Horizontal	West	5	3					
Horizontal	South	5	2					
Horizontal	East	5	3					
Horizontal	North	5	3					
Vertical	West	3	5	3	1	3	3	2
Vertical	South	3	5	3	3	3	2	2
Vertical	East	3	5	3	2	3	2	2
Vertical	North	3	5	3	2	3	2	2
Horizontal	West	3	3					
Horizontal	South	3	3					
Horizontal	East	3	3					
Horizontal	North	3	1					
Vertical	West	1	3	3	1	3	2	2
Vertical	South	1	3	3	2	3	2	1
Vertical	East	1	3	3	1	2	2	2
Vertical	North	1	3	3	1	5	3	2
Horizontal	West	1	2					
Horizontal	South	1	1					
Horizontal	East	1	2					
Horizontal	North	1	1					
Vertical	West	0.5	2	3	1	2	2	
Vertical	South	0.5	2	3	1	2	1	
Vertical	East	0.5	2	3	1	2	1	
Vertical	North	0.5	2	3	0	2	2	
Vertical	West	0.1	1	3	1	0	2	
Vertical	South	0.1	1	3	1	1	0	
Vertical	East	0.1	1	3	1	1	2	
Vertical	North	0.1	1	3	0	2	2	

- 0 Unintelligible
- 1 Just barely intelligible
- 2 Intelligible with much static
- 3 Intelligible with some static
- 4 Clear with a little static
- 5 Clear with no static

Table 2 shows the intelligibility of the reception as a function of the distance between transmitter and receiver. On the minute, DVM, with the standard long-whip antenna vertically polarized, transmitted the time. On the half-minute, RCA transmitted the time. The frequency was held constant at 63.9 MHz. The power to the antennas was held constant at 5 W. RCA walked slowly north from Building 323 and then returned. The distances are interpolated from the known starting and ending locations.

Table 2. Record of transmissions between DVM at the lighthouse at Cabrillo Point and RCA walking along Woodward Road.

Time (6/25/01)	DVM Received	RCA Received	Distance (m)	Comments
1328	Clear	Clear	3573	Start from Building 323
1329	Clear	Clear	3600	
1330	Clear	Clear	3627	
1331	Clear	Clear	3654	
1332	Broken but intelligible	Clear	3681	
1333	No	Clear	3708	
1334	No	Just barely	3735	Going behind hill
1335	No	No	3762	Standard antenna also has poor reception
1336	Broken but intelligible	Clear	3789	
1337	Broken but intelligible	Clear	3816	
1338	No	Just barely	3843	
1339	No	Just barely	3870	
1340	Broken but intelligible	Clear	3897	Beyond hill
1341	No	Clear	3924	
1342	No	Just barely	3951	
1343	Just barely	Just barely	3978	
1344	No	Just barely	4005	
1345	No	Just barely	4032	
1346	No	Just barely	4059	
1347	No	No	4086	Turn-in road behind second hill
1348	No	Just barely	4113	
1349	No	Just barely	4140	
1350	No	Just barely	4167	
1351	No	Just barely	4194	
1352	No	Just barely	4221	
1353	No	Just barely	4248	
1354	Broken but intelligible	Just barely	4275	
1355	No	No	4302	

Table 2. Record of transmissions between DVM at the lighthouse at Cabrillo Point and RCA walking along Woodward Road. (continued)

Time (6/25/01)	DVM Received	RCA Received	Distance (m)	Comments
1356	No	No	4329	
1357	No	No	4356	
1358	No	No	4383	
1359	Broken but intelligible	Just barely	4410	
1400	No	Clear	4437	Beyond influence of hill
1401	Broken but intelligible	Clear	4464	
1402	No	Clear	4481	
1403	Clear	Clear	4508	End of road
1408	No	Clear	4508	Start back
1409	Clear	Clear	4481	COMWIN facing DVM
1410	Clear	Clear	4454	
1411	No	Clear	4427	
1412	Broken but intelligible	Clear	4410	
1413	Broken but intelligible	Clear	4383	
1414	No	Clear	4356	
1415	No	Just barely	4329	
1416	No	No	4302	
1417	No	Just barely	4275	
1418	No	Clear	4248	
1419	No	Just barely	4221	
1420	No	Just barely	4194	
1421	No	Just barely	4167	
1422	No	Just barely	4140	
1423	No	Just barely	4113	
1424	No	Just barely	4086	
1425	No	Just barely	4059	
1426	No	Just barely	4032	
1427	No	Just barely	4005	
1428	No	No	3978	
1429	No	Clear	3951	
1430	No	Just barely	3924	
1431	No	Clear	3897	
1432	No	Just barely	3870	
1433	No	Just barely	3843	
1434	No	Just barely	3816	
1435	No	Just barely	3789	
1436	No	No	3762	
1437	No	No	3735	Emerging from behind hill
1438	No	No	3708	
1439	No	Just barely	3681	
1440	No	Clear	3654	
1441	No	Clear	3627	
1442	No	Just barely	3600	
1443	No	Clear	3573	End at Building 323

The intelligibility of the reception seemed to be slightly dependent on distance, but more strongly dependent on the terrain. There was an asymmetry concerning the reception by the long-whip antenna than from the vest antenna. DVM could not hear a transmission from the vest antenna nearly as well as RCA could hear from the long-whip antenna. The transmission when the antenna was facing the recipient was much worse than when the vest antenna was facing away.

Table 3 shows that DVM was located on one of the highest points on Point Loma, the JTIDS tower. The geographical location of this tower is 32° 41.350'N, 117° 14.835'W. RCA accompanied by John Strauch of SSC San Diego, who wrote down the observations and recorded the GPS data, walked west and then north on Woodward Road. DVM called out the time every 2 minutes. RCA transmitted the time 1 minute later. RCA started walking from the Model Range at 1202 and continued walking until 1236, when he turned around and started back. The experiment ended at 1256 at the base of the hill that goes east along Woodward Road. The JTIDS tower is at an altitude of 121 m. The minimum height above sea level that RCA walked was 40 m near the end of Woodward Road.

Table 3. Record of transmissions between RCA using COMWIN vest antenna and DVM using standard antenna for PRC-148 radio.

Time (6/26/01)	Latitude Minutes North of 32°	Longitude Minutes West of 117°	Distance (m)	RCA Received	DVM Received
1202	41.874	14.889	976	Clear	Clear
1204	41.815	14.867	864	Clear	Clear
1206	41.747	14.864	738	Clear	Clear
1208	41.659	14.893	580	Clear	Clear
1210	41.610	14.980	533	Clear	Clear
1212	41.658	15.070	679	Clear	Clear
1214	41.729	15.128	839	Clear	Clear
1216	41.811	15.155	991	Clear	Clear
1218	41.882	15.224	1159	Clear	Clear
1220	41.891	15.232	1180	Clear	Clear
1222	42.004	15.231	1362	Clear	Clear
1224	42.036	15.218	1406	Clear	Clear
1226	42.127	15.209	1555	Clear	Clear
1228	42.215	15.235	1722	Clear	Clear
1230	42.304	15.246	1883	Clear	Clear
1232	42.391	15.238	2031	Clear	Clear
1234	42.451	15.288	2162	Clear	No
1236	42.455	15.312	2181	Clear	No
1238	42.388	15.264	2039	Clear	Clear
1240	42.365	15.242	1987	Clear	Low
1242	42.277	15.241	1833	Broken up	No
1244	42.199	15.236	1695	Broken up	No
1246	42.118	15.208	1539	Broken up	No
1248	42.039	15.216	1410	Low	No
1250	41.958	15.250	1301	Low	No
1252	41.879	15.220	1151	Clear	Clear
1254	41.812	15.155	992	Clear	Clear
1256	41.726	15.128	834	Clear	Clear

There was a continued asymmetry between the two antennas. The ability of the long-whip antenna to transmit and the vest antenna to receive was better than with the roles reversed. This issue will be investigated thoroughly in FY 2002.

The final experiment conducted with the radios kept the distance between transmit and receiver small (320 m). Table 4 shows the quality of the reception as a function of the relative orientation of the transmitter and receiver. DVM oriented the standard antennas either vertically or toward one of the cardinal points. RCA with the vest antenna was always vertical, but faced one of the four cardinal points. The power was kept fixed at 0.1 W. The distance between sender and receiver was kept fixed at 320 m. DVM changed antennas from the long-whip antenna to the short-whip antenna for frequencies above 63.9 MHz. DVM was north of RCA.

There are several differences between changing the polarization of a linear dipole antenna from vertical to horizontal while keeping the COMWIN antenna vertical and vice versa. The propagation characteristics of the signal over land depend on the polarization. The second difference is that the impedance of the antenna depends upon the proximity to the ground. Nonetheless, these results show that the COMWIN antenna can receive the cross-polarized signal with acceptable quality.

The results of the radio tests showed that the vest antenna had approximately the same capability as the standard antenna. The gain of the antennas was comparable. Terrain was the primary factor that determined the range of reception and intelligibility of the signal. During FY 2002, more study will be done on quantifying this relationship.

Table 4. Quality of reception of a signal of a particular frequency and polarization.

DVM Polar.	RCA Dir.	DVM Dir.	RCA 63.9	RCA 139.3	RCA 226.5	RCA 258.5	RCA 337.5	RCA 435.1	DVM 63.9	DVM 139.3	DVM 226.5	DVM 258.5	DVM 337.5	DVM 435.1
V	V	N	4	4	3	4	3	3	5	5	3	4	3	3
V	V	W	4	5	3	4	4	3	5	5	4	3	3	3
V	V	S	4	4	4	4	4	3	5	4	3	3	3	3
V	V	E	4	4	3	3	4	3	5	4	3	2	3	3
H	N	N	3	3	2	1	2	2	3	3	3	4	3	2
H	W	N	3	3	2	2	3	2	4	3	3	4	4	3
H	S	N	4	4	3	3	3	3	4	2	4	3	4	3
H	E	N	4	4	3	1	3	3	3	3	4	3	4	2
H	N	W	3	3	2	3	3	2	3	3	3	2	3	3
H	W	W	3	3	2	3	4	2	3	4	4	2	2	3
H	S	W	3	3	2	3	3	2	4	3	4	3	3	2
H	E	W	3	3	3	3	4	2	4	2	4	3	3	2
H	N	S	3	3	3	5	2	2	3	3	3	3	3	3
H	W	S	3	3	3	3	2	2	3	3	1	3	3	3
H	S	S	3	3	3	3	3	3	4	3	2	3	4	3
H	E	S	3	3	3	3	3	2	4	2	3	3	3	2
H	N	E	4	3	2	3	3	3	4	3	3	3	3	3
H	W	E	4	3	2	3	3	3	4	3	3	2	4	3
H	S	E	4	3	2	3	3	3	4	3	2	3	4	3
H	E	E	4	3	3	3	3	3	4	3	3	3	4	2

- 0 Unintelligible
- 1 Just barely intelligible
- 2 Intelligible with much static
- 3 Intelligible with some static
- 4 Clear with a little static
- 5 Clear with no static
- DVM Initials of person receiving signal
- RCA Initials of person receiving signal
- V Vertical
- H Horizontal

- N North
- S South
- E East
- W West

HELMET ANTENNA

The helmet antenna is an important element of the COMWIN system. There is some overlap in the frequency coverage between the helmet and the vest antenna. The vest covers the 30- to 500-MHz range while the helmet covers the 400- to 2000-MHz. The helmet antenna was tested up to a frequency of 2400 MHz. The helmet antenna should cover the frequency ranges that the vest does not cover very well.

Figures 12 and 13 show the Mark III helmet antenna. The elements that distinguished the newest version from the Mark I fabricated by NPS (Adams et al., 2000) were the imposition of symmetry on the basic design and the breaking of symmetry to match the impedance to a 50-ohm load. A capacitor was also used for matching. The symmetry was imposed by using a gap at the top of the antenna (figure 12). The strips of FlecTron[®] that form the antenna are of approximately equal width (figure 12). The lack of gain in the Mark II version compared to the Mark I showed that the gap should be horizontal and very small. The value of the 7.5-pf capacitor (put into the circuit in series with the feed) was chosen to make the best match (figure 13).



Figure 12. Mark III helmet antenna (front).



Figure 13. Mark III helmet antenna (rear).

The symmetry was not absolute. The helmet is longer front to back than side to side. Experiments also showed that if a second shorting strap were asymmetrically placed (at about 2 o'clock, where the feed is at 6 o'clock and the first shorting strap is at noon), the matching would be improved. Figure 12 shows the asymmetrically placed shorting strap.

IMPEDANCE/VSWR MEASUREMENTS

We used the Anritsu[®] Sitemaster to conduct most of the initial measurements to determine the optimum match. The Sitemaster can go to a frequency as high as 1200 MHz. To cover the more extended range of 400 to 2000 MHz, we used a HP 8510C network analyzer. Figure 14 presents the VSWR versus frequency of the antenna. The VSWR was almost always less than 3:1 for all frequencies between 400 and 1700 MHz. Even for frequencies as high as 2000 MHz, the VSWR was not very large. Unlike the vest antenna, the presence of the person on the helmet version did not have a dramatic effect on the impedance. The VSWR of the helmet antenna on a desk increased slightly compared to the VSWR with a person wearing the helmet antenna. The Kevlar helmet had only a small effect on the VSWR.

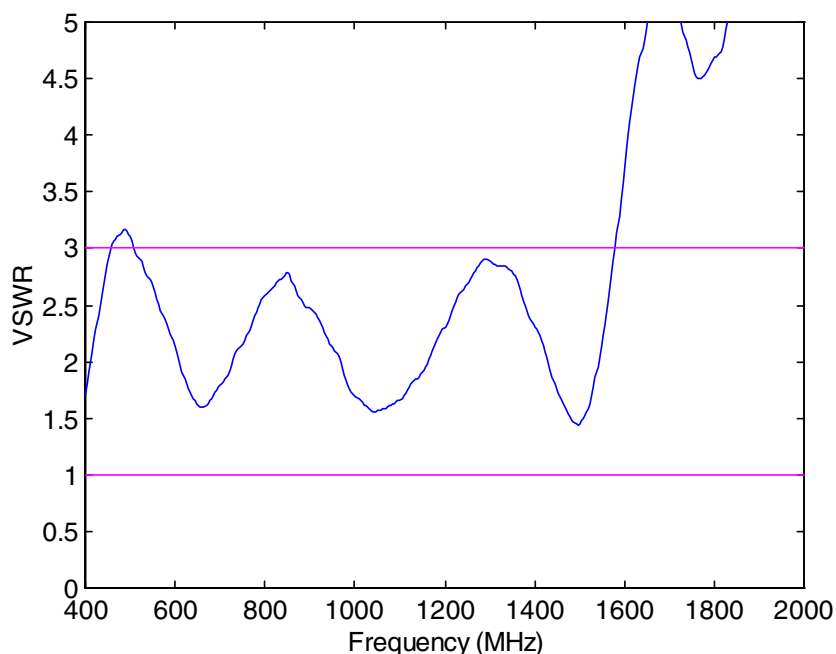


Figure 14. VSWR versus frequency of Mark III helmet antenna worn by a person.

ANTENNA MEASUREMENTS

As in the case of the vest antenna, the measurements included gain at boresight for vertical and horizontal polarization and radiation patterns in the azimuth and elevation planes. All these measurements were made in the SSC San Diego Anechoic Chamber (Building 377). The signal generator, spectrum analyzer, and standard gain antenna were the same as those described above. A Mini-Circuits® low-noise amplifier increased the signal by 30 dB. The transmit antenna was a dipole antenna with an orientation that could be readily changed to radiate either vertically or horizontally polarized energy.

Figure 15 shows the gain at boresight for vertical and horizontal polarizations of the helmet antenna. The frequencies at which the gain was measured varied from 400 to 1790 MHz in steps of 5 MHz. For most frequencies greater than 800 MHz, the vertical gain was greater than the horizontal one. For frequencies near 400 MHz, the horizontal polarization dominated. For a few frequencies, the values of the gain for horizontal were equal to that for vertical. If the feed of the antenna were properly configured, the polarization could become circular. The maximum gain was slightly greater than 0 dBi (1000 MHz). The minimum gain at boresight was -21 dBi (1800 MHz). The gain had a somewhat oscillatory character.

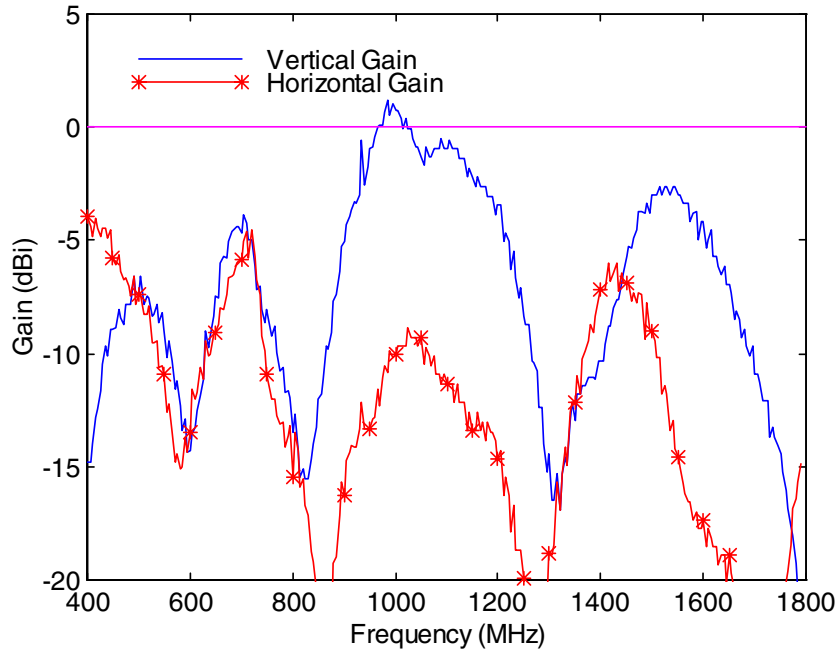


Figure 15. Gain of Mark III helmet antenna in vertical and horizontal polarizations.

Figure 16 shows the radiation patterns in the azimuth direction for the frequencies 500 to 1800 MHz in steps of 100 MHz. A spectrum analyzer measured the patterns in the same way as those for the vest antenna.

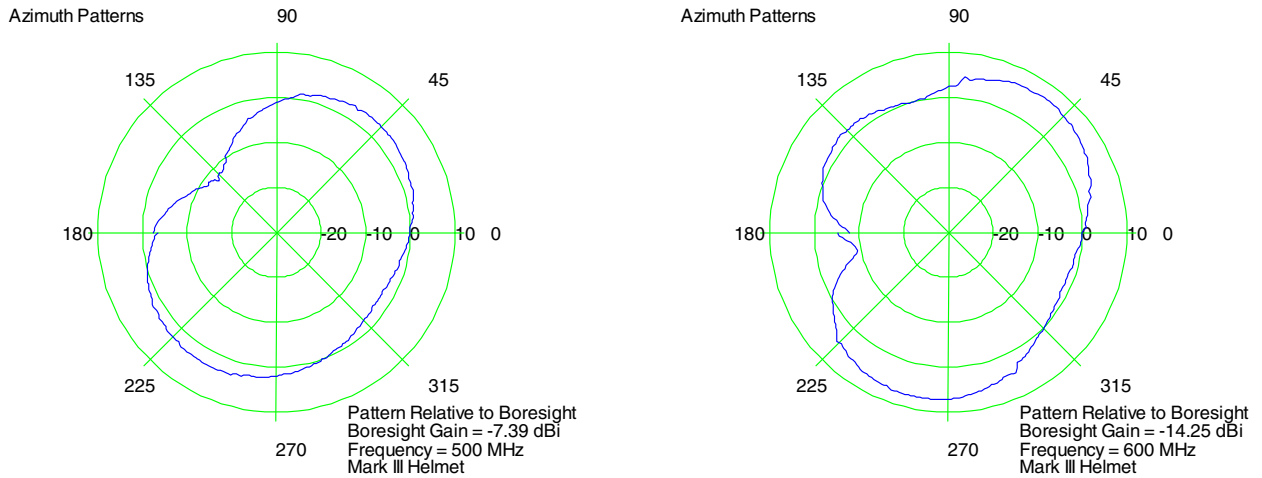


Figure 16. Azimuth radiation patterns for Mark III helmet antenna at frequencies of 500 to 1800 MHz in steps of 100 MHz.

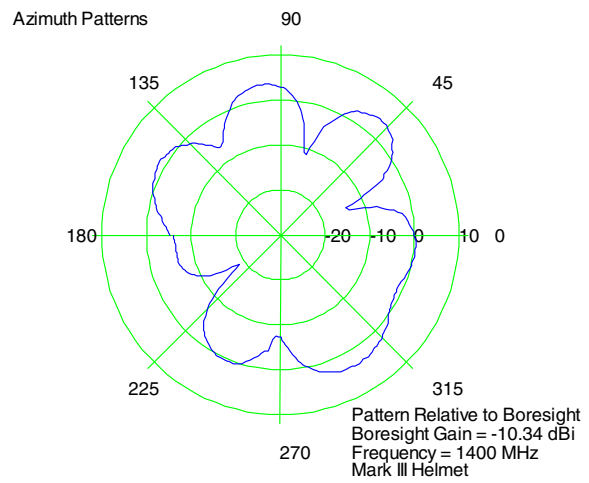
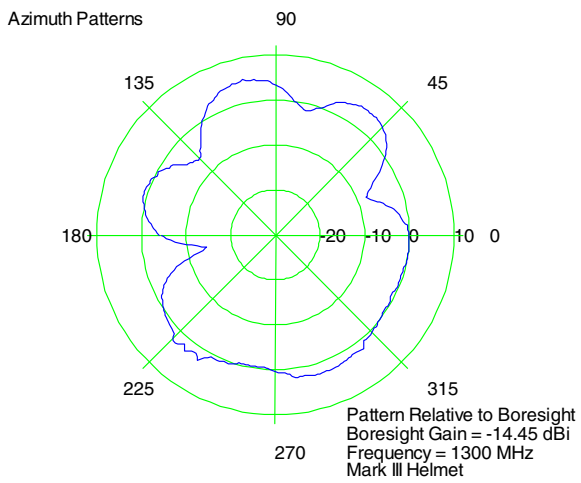
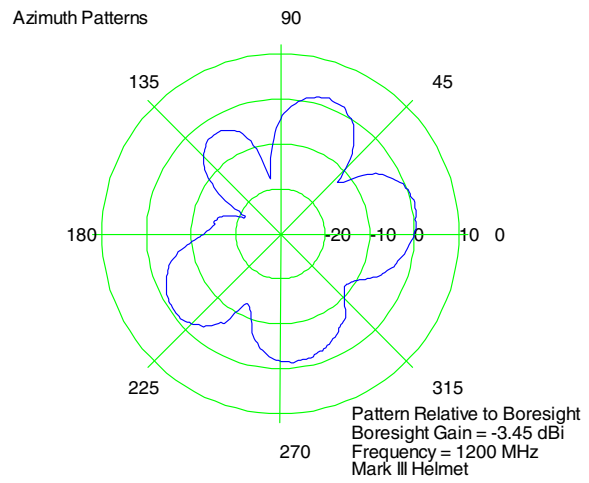
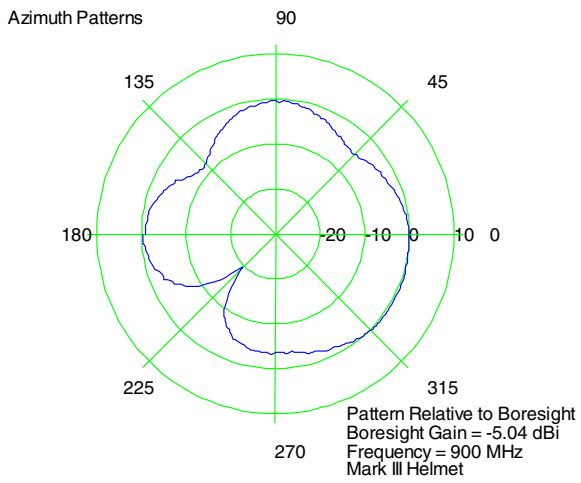
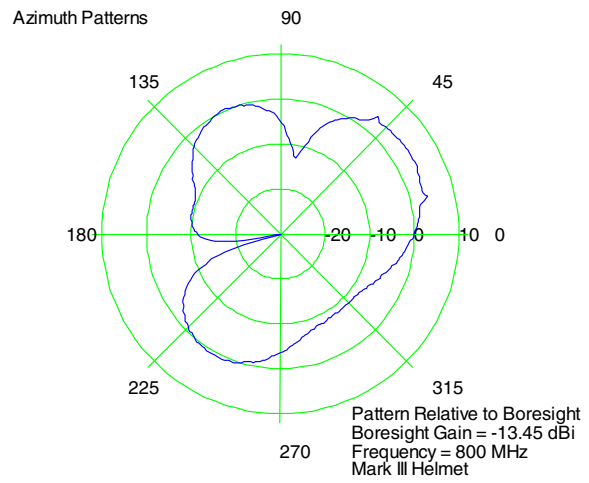
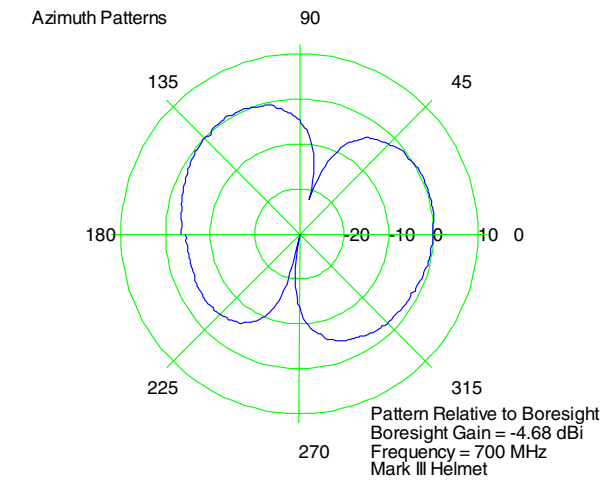


Figure 16. Azimuth radiation patterns for Mark III helmet antenna at frequencies of 500 to 1800 MHz in steps of 100 MHz. (continued)

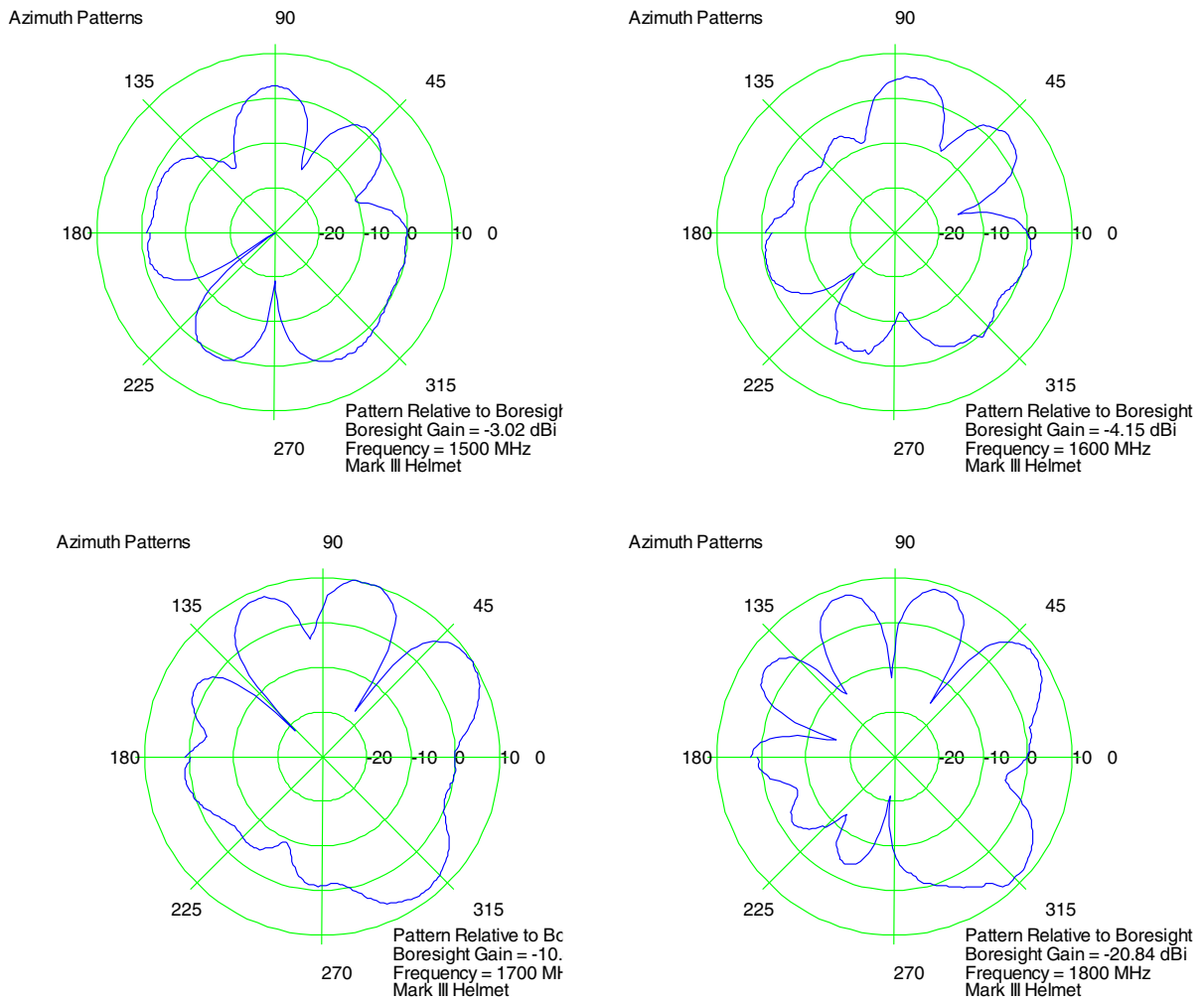


Figure 16. Azimuth radiation patterns for Mark III helmet antenna at frequencies of 500 to 1800 MHz in steps of 100 MHz. (continued)

As figure 16 shows, the number of lobes in the patterns increases as the frequencies increase. Each pattern was normalized to the power received at boresight.

Figure 17 shows the pattern in the elevation direction when the azimuth angle was 0°. Figure 18 shows the radiation pattern in the elevation when the azimuth angle was 90°. Similar to the azimuth patterns, the amplitudes were normalized to the amplitude at boresight.

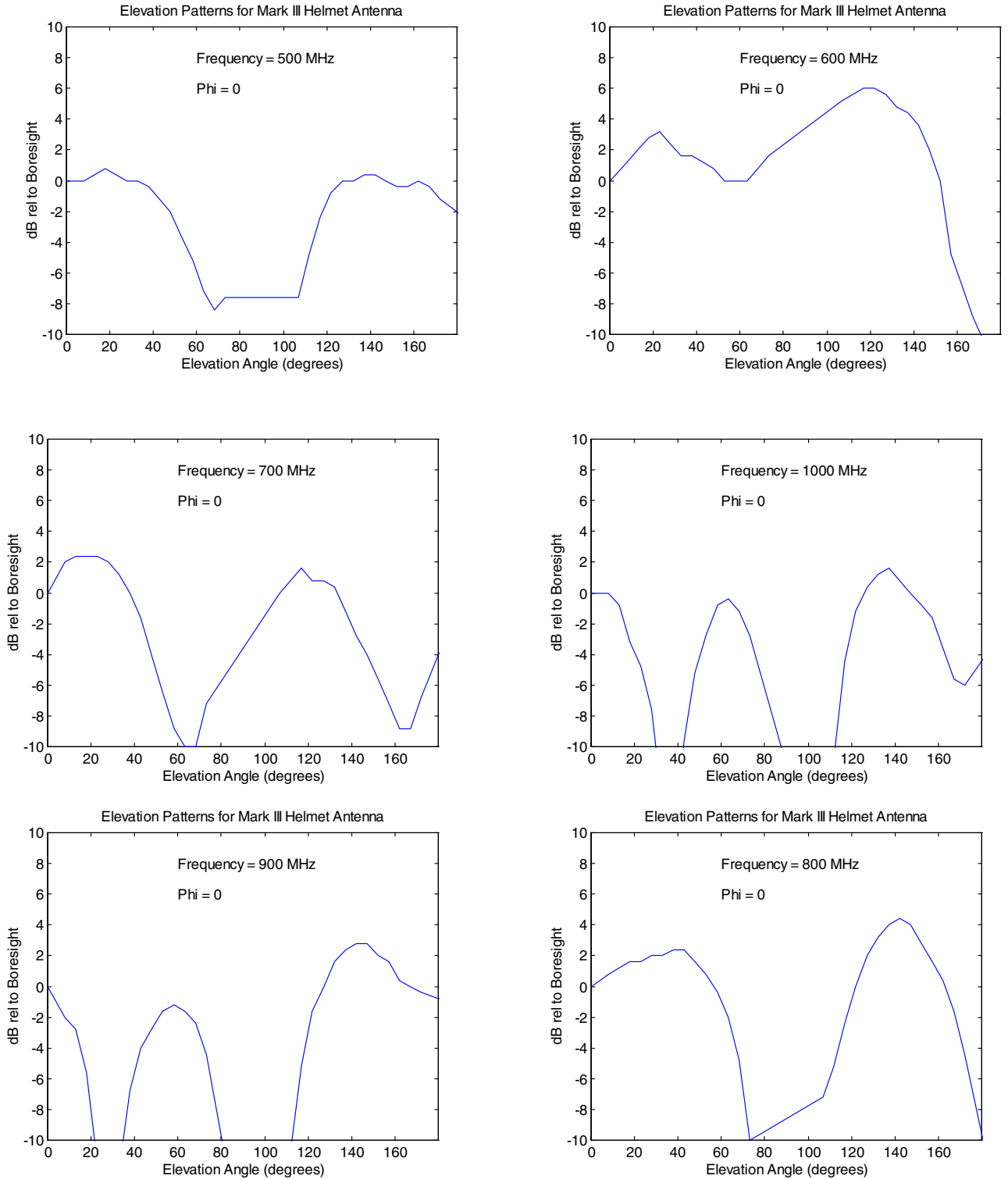


Figure 17. Elevation radiation patterns for Mark III helmet antenna at frequencies of 500 to 1800 MHz in steps of 100 MHz for an azimuth angle of 0° .

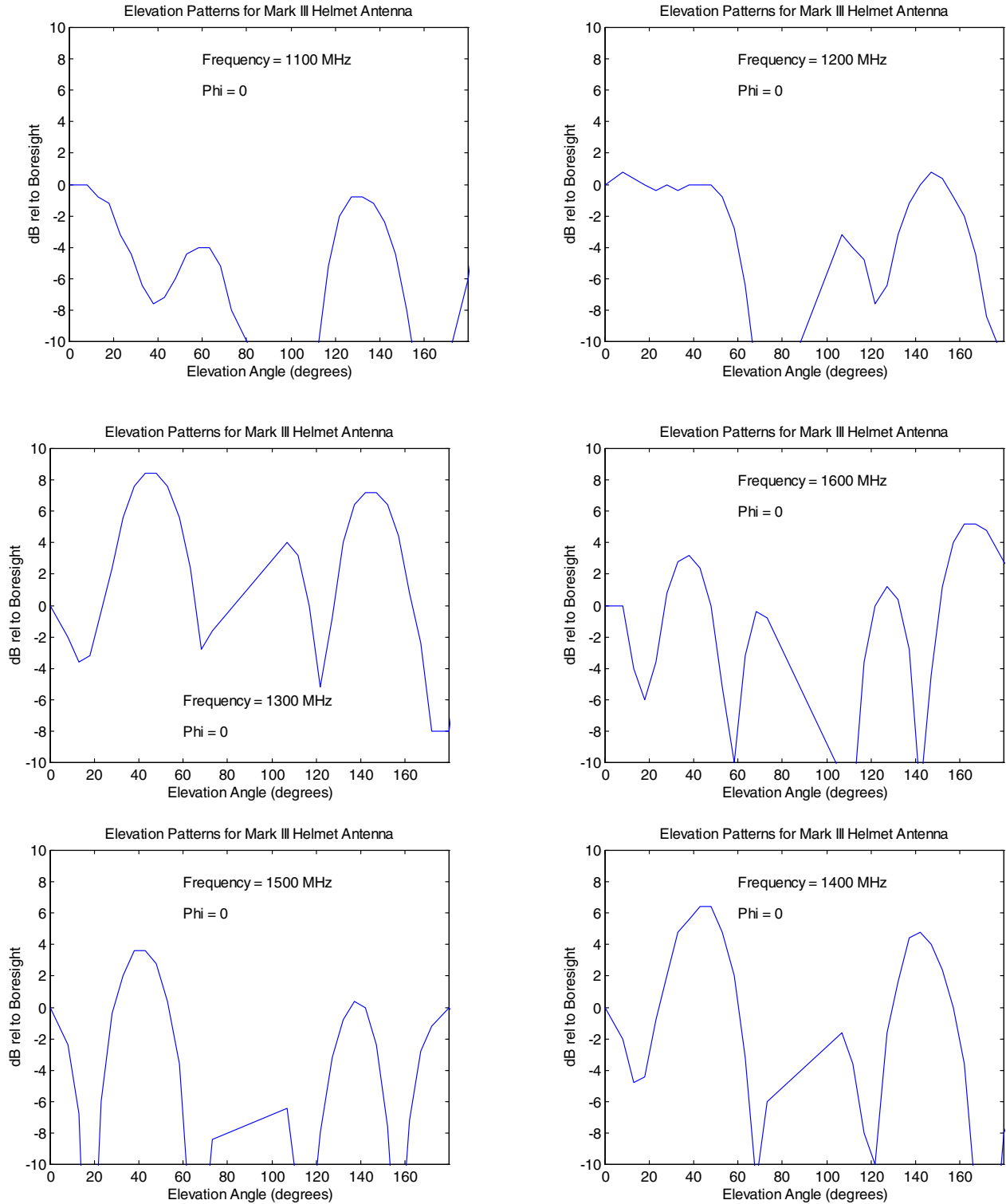


Figure 17. Elevation radiation patterns for Mark III helmet antenna at frequencies of 500 to 1800 MHz in steps of 100 MHz for an azimuth angle of 0° . (continued)

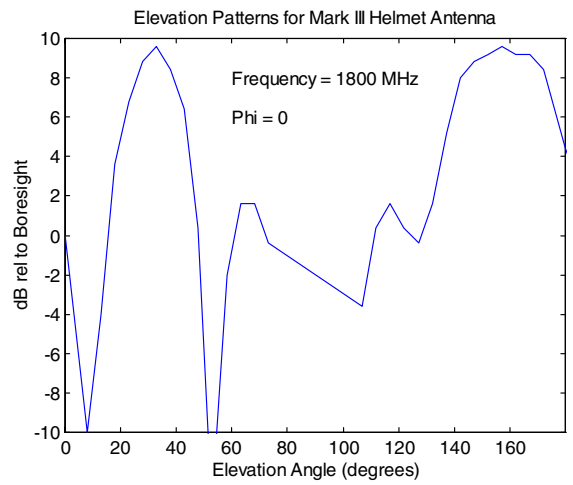
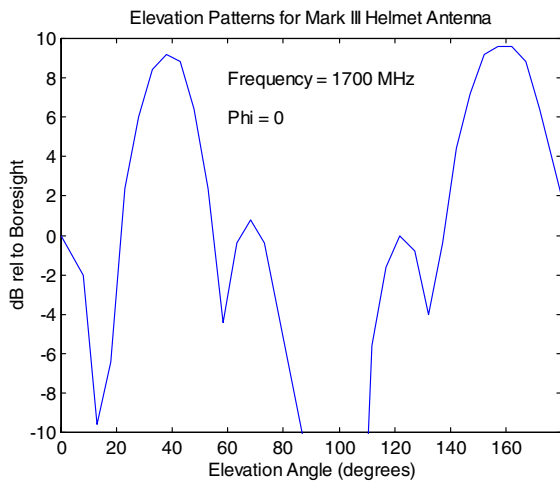


Figure 17. Elevation radiation patterns for Mark III helmet antenna at frequencies 500 to 1800 MHz in steps of 100 MHz for an azimuth angle of 0°. (continued)

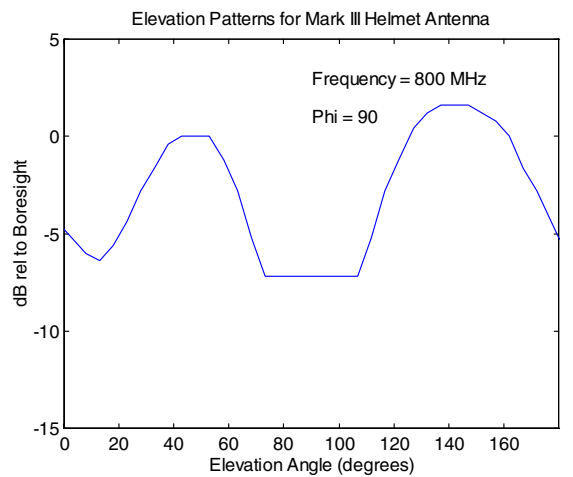
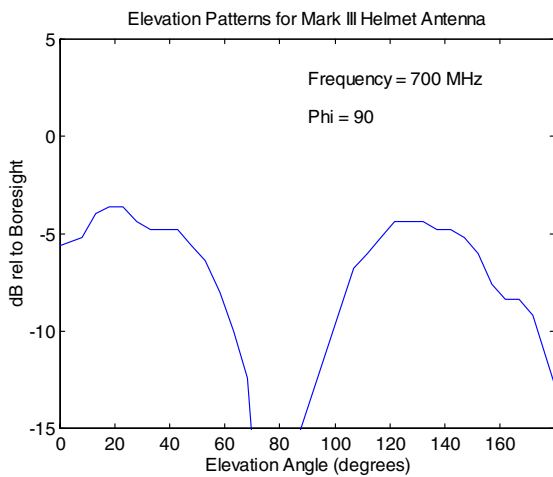
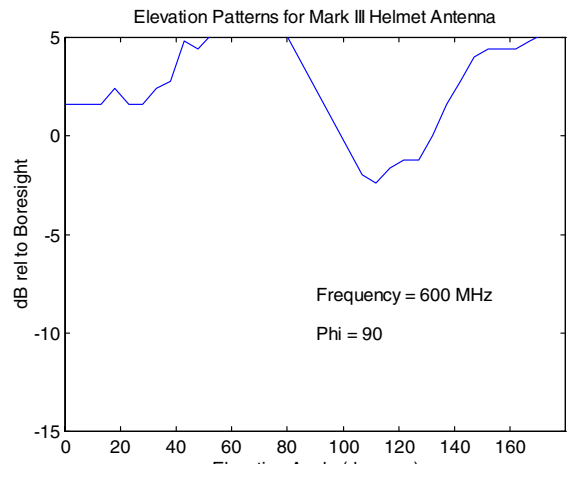
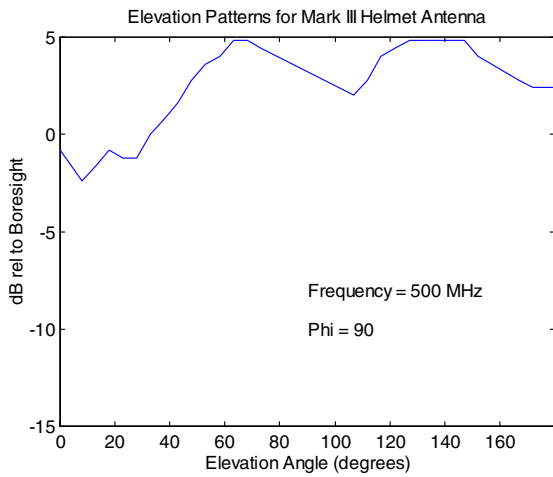


Figure 18. Elevation radiation patterns at frequencies of 500 to 1800 MHz in steps of 100 MHz for azimuth angle of 90°.

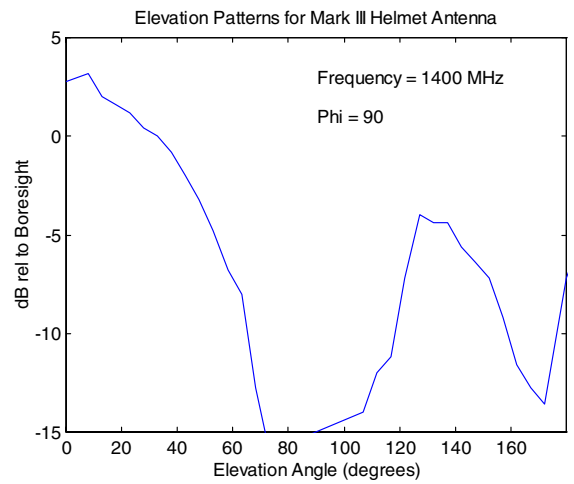
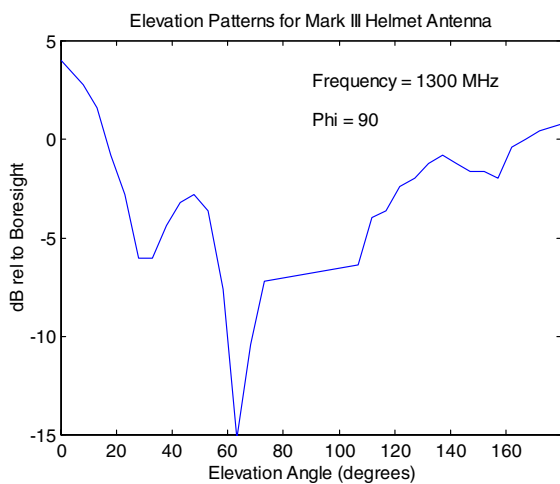
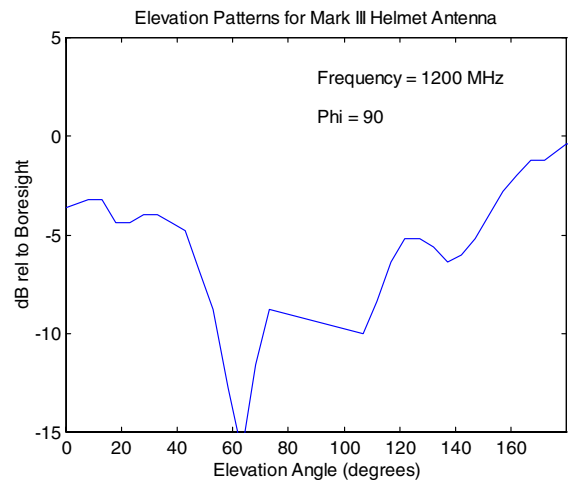
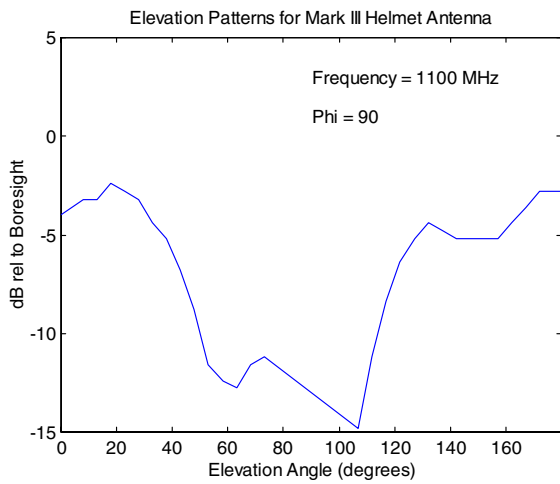
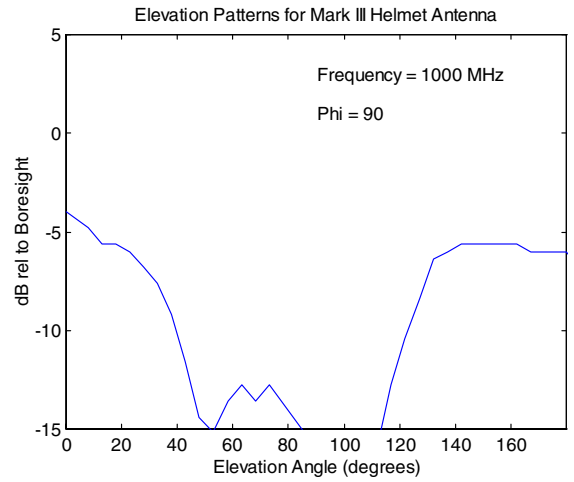
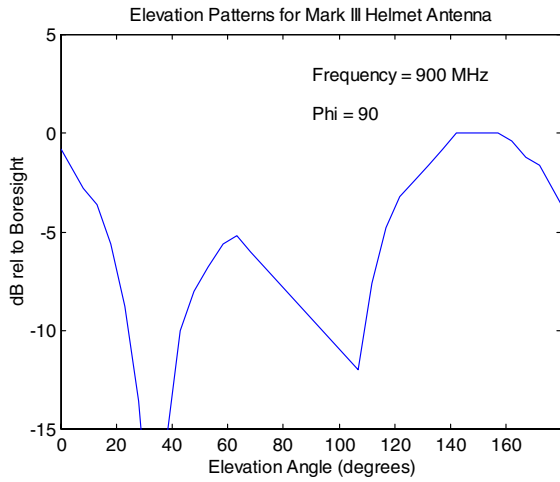


Figure 18. Elevation radiation patterns at frequencies of 500 to 1800 MHz in steps of 100-MHz for an azimuth angle of 90° . (continued)

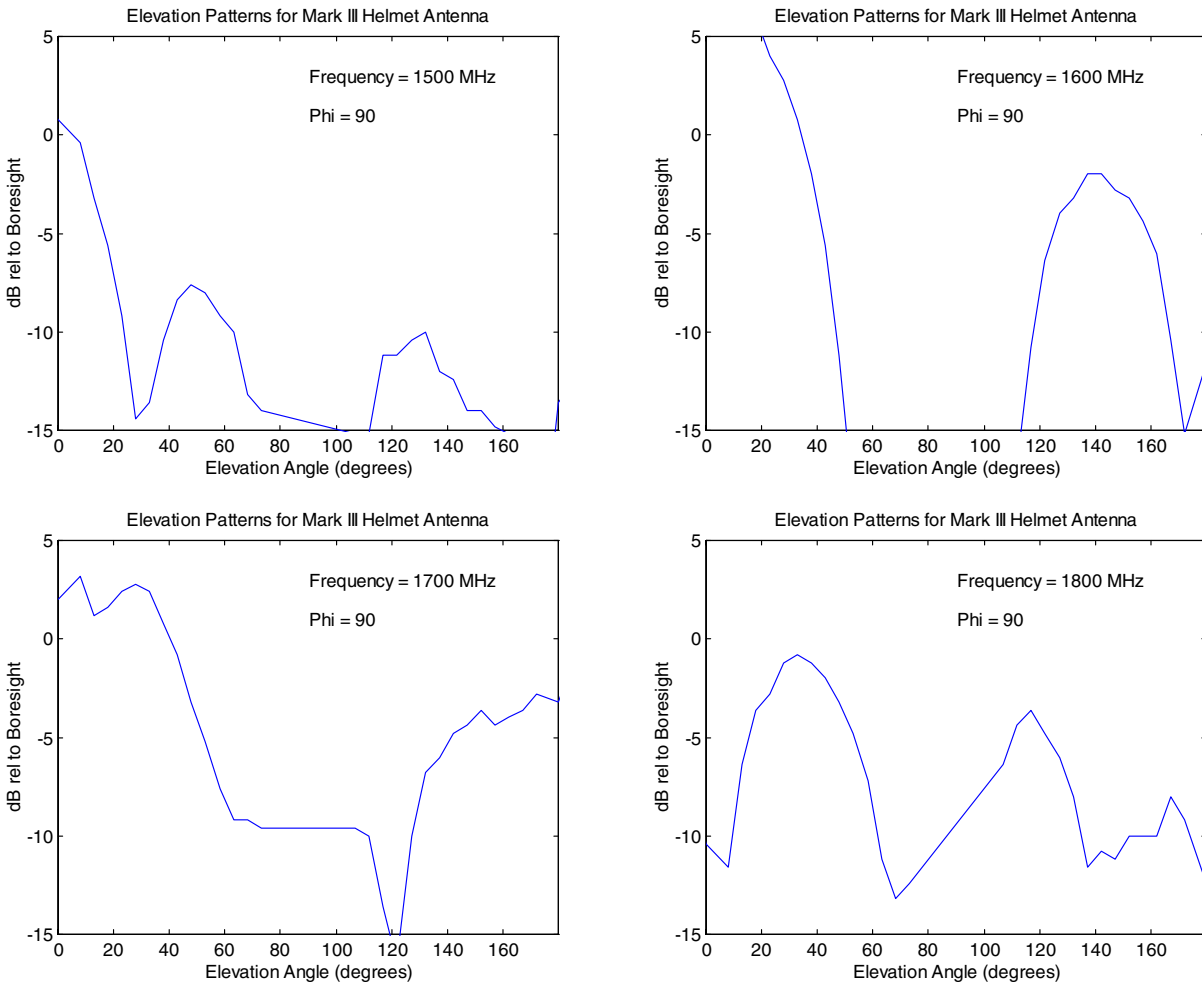


Figure 18. Elevation radiation patterns at frequencies of 500 to 1800 MHz in steps of 100 MHz for an azimuth angle of 90°. (continued)

The helmet antenna has lobes in the elevation pattern at virtually all frequencies. The appearance of lobes is probably caused by the non-circular nature of the helmet itself. The lobes can be exploited to provide higher gain.

VIDEO DATA TRANSFER TESTS

As an example of using the helmet antenna for receiving data, an experiment using a wireless local area network (LAN) with an 802.11 protocol was set up. The wireless LAN transmitted at data rates of up to 11 Mbps at a frequency of 2.4 GHz. The LAN was set up with a transmit and receive antenna as a microstrip line. Transmit power could not be controlled. The LAN had a quality control feature that determined the optimum data transfer rate. If the bit-error rate got too large for the data rate and link margin, the data transfer rate decreased by a factor of 2 down to a minimum of 1.3 Mbps. Thus, not just a blank screen characterized a failing link margin, but also a scene that did not change continuously because of decreasing data transfer rate. This data transfer rate was illustrated by the image of the second hand of a clock. If the link margin was good, the second hand, which moved continuously, appeared to move at 1-s increments. As the link margin changed to unacceptable, the second hand appeared to move at 2-, then 5-s increments. As the link margin

decreased further, the motion froze. A further decrease in the link margin caused the screen to go blank. One of the windows of the wireless LAN software also had the link margin in dBm.

An experiment was conducted at the Building 427 tower. This tower, made of wood, is approximately 10-m high and open to the sky. A camera facing the second hand of a clock was placed on the tower. The camera was connected to the wireless LAN, which had a microstrip antenna acting as a transmitter. The receiving antenna (also a microstrip) of the wireless LAN was inserted into a laptop computer. The microstrip antenna had a port for insertion of the output from another source. In the immediate vicinity of the camera, the second hand of the clock moved in increments of 1 s. At a distance of 30 m from the tower, this motion was in increments of 2 s. At 40 m, the increment was 5 s. At a distance of 60 m (measured by a GPS receiver), the motion froze. Moving the laptop slightly in the horizontal plane caused the picture to go black. The link margin was negative.

At the 60-m distance of the clock from the laptop, the output of the helmet antenna was inserted into the port of the microstrip attached to the laptop. The image of the clock immediately changed to the correct time. The second hand moved in increments of 1 s again. Moving the laptop to the edge of the SSC San Diego Model Range near the entrance to Building 375 caused the second hand to move at 5-s increments. The distance between the clock and laptop was 160 m.

Figure 19 shows a photograph taken during the experiment. In the background (approximately 60 m away) is Building 427 with a camera facing a clock outputting an image along a 2.4-GHz wireless LAN. This location is where the microstrip antenna failed to provide a sufficient link margin. The helmet antenna worked at 100 meters beyond this location.



Figure 19. Helmet antenna transferring video data.

Changing the orientation of the transmitting microstrip antenna (the wireless LAN box was turned on its side) decreased by a factor of 2 the effective range by the microstrip and helmet antenna. The experiment was also conducted in the hallway of Building 382. If the wireless LAN was at the end of a hallway and the laptop computer was in one of the rooms, there was only a blank screen because of the metallic construction of the walls. Putting the helmet antenna on a chair in the hallway but attached to the laptop in the room caused the image to again move at the 1-s increments. Changing the orientation of the helmet antenna caused changes in the increment of motion of the second hand. This change illustrated the presence of lobes and nulls in the pattern of the helmet antenna.

WHOLE-BODY ANTENNA

In December 1999, Professor Lebaric suggested a method to efficiently transmit or receive signals in the 2- to 30-MHz frequency range. Because a person's body is much smaller than a typical wavelength in this band, the mismatch is likely to be severe. The mismatch changes if the ground serves as part of the antenna. Accordingly, Lebaric suggested a scheme in which the signal is fed near the neck and goes down a conductive path to the soles of the feet. Shoe inserts were made of FlecTron[®]. The signal was capacitively coupled to the ground. The ground completed the circuit. The antenna could then be long enough that the antenna could be efficiently matched to the feed.

Figure 20 shows the front view of the whole-body antenna. The vest antenna (the Mark II fabricated during FY 2000) formed a reflecting plane. The flak jacket kept the signal from shorting out because of the action of the vest antenna. Figure 21 shows the rear view of the whole-body antenna. The feed near the middle of the back connected to two strips of conductive cloth. The path was down the sides of the flak jacket. Snaps connected these conductive strips to the ones on the sides of the pants. These, in turn, connected to the shoes. In the realistic case, the strips would be on the inside of the cloth of the flak jacket and pants so that a sniper could not see them. Socks with conductive soles could be used rather than the bottoms of shoes.



Figure 20. Whole-Body antenna (front view).

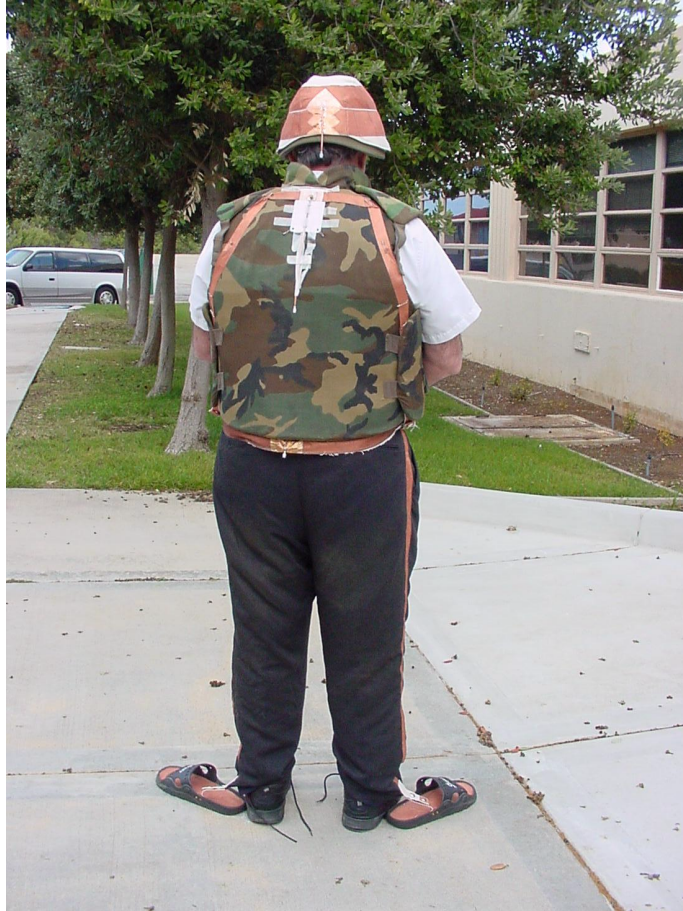


Figure 21. Whole-Body antenna (rear view).

IMPEDANCE/VSWR MEASUREMENTS

The portability of the Sitemaster allowed impedance and VSWR measurements to be done in various locations. The measurement sites included a ground plane (on the SSC San Diego Model Range), under a tree (where metal is unlikely), on a sidewalk, and inside a room. The Sitemaster has a minimum frequency of 5 MHz.

The measurements indicated that the addition of a 4:1 RF transformer would cause an efficient match between the antenna and the feed. Accordingly, a Mini-Circuits[®] transformer, advertised as providing a factor of 4 reduction in impedance in the 0.2- to 600-MHz frequency range, was purchased. The only difficulty with the device was that the maximum power allowed was 0.25 W (Mini-Circuits[®], 1997, p. 14-6). Thus, high-power signal transmission and radiation-hazard studies of this antenna will have to await the manufacture of a device that can stand as much as 5 W of input power.

Figure 22 shows the VSWR versus frequency of the whole-body antenna when the wearer was located on a sidewalk and on a ground plane. The data were obtained after the transformer was inserted into the circuit. The VSWR of the whole-body antenna was extremely low, less than 2:1 in the 5- to 30-MHz frequency range. Such a good matching was completely unexpected. The difference in VSWR between the wearer on a ground plane and sidewalk was small. This smallness was probably caused by the large loss introduced into the system by the interaction of the person with the antenna.

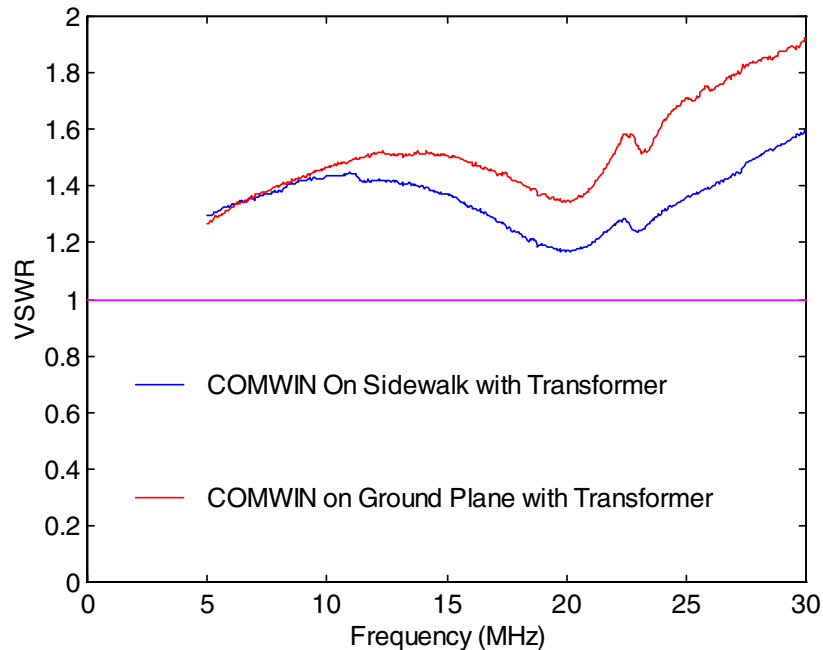


Figure 22. VSWR versus frequency for whole-body antenna.

ANTENNA MEASUREMENTS

The pattern measurement was not attempted because the wavelength was extremely large at high frequency (HF). We assumed that the pattern was relatively isotropic in the azimuthal plane. The small electrical size of the antenna would certainly imply such a conclusion. Fortunately, SSC San Diego has the mechanism to compare the signals from an HF antenna with those from a 35-foot whip antenna, the standard Navy shipboard antenna for the 2- to 30-MHz range. The method of measurement was a comparison of the transmission coefficient as determined by a Hewlett Packard® 8510 C network analyzer. High loss implies that the antenna will not transmit or receive an HF signal well. The comparison is a measure of antenna gain. Figure 23 shows this comparison measured on a ground plane at the SSC San Diego Model Range. On the graph, an average of the measurement over 13 frequencies was used to smooth the result. At a frequency of more than 20 MHz, the whole-body antenna was nearly as capable as the 35-foot whip antenna. At frequencies below 10 MHz, the whole-body antenna is poor compared to one with a resonant frequency that is approximately 7 m (1/4 wavelength because the whip antenna is used as a monopole).

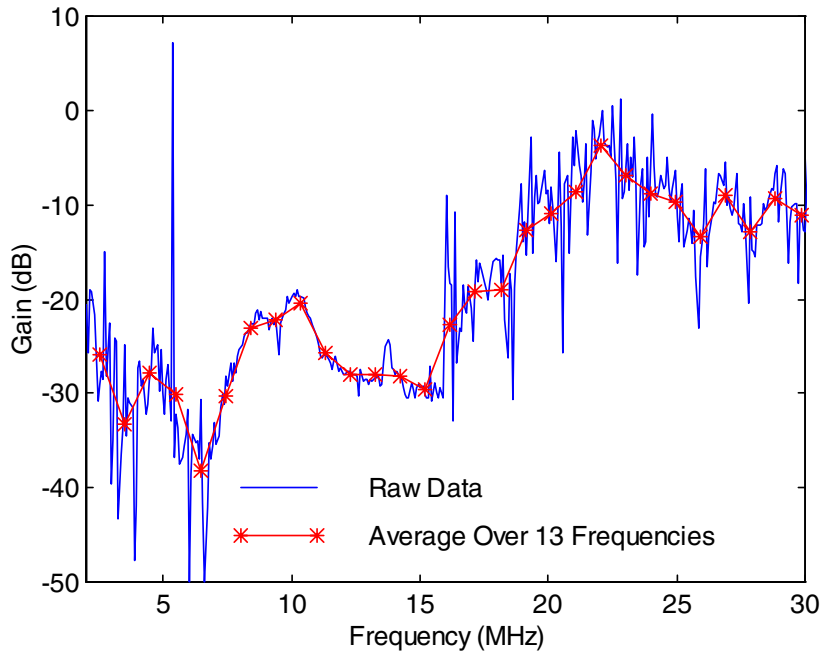


Figure 23. Gain of whole-body antenna compared to 35-foot whip antenna.

RADIO TESTS

Station WWV broadcasts from Boulder, CO, at frequencies of 5, 10, 15, and 20 MHz. The signal broadcast is a steady beep, beep, beep... at 1-s intervals. The time in Greenwich is broadcast every minute. This signal tests HF antennas because of the signal's predictability. HF propagation is notorious for variability caused by the ionosphere, which reflects the signal and causes interference. Certain bands in the below 10-MHz frequency range are unusable one day, but crystal clear the next, because of these effects.

On 7 February and on 13 June 2001, the whole-body antenna was used with an Interior Communications Systems (ICOM) receiver model IC-R8500. This receiver could be tuned digitally in small increments in the 2- to 30-MHz range. The experiment on 7 February was conducted on the ground plane. The experiment on 13 June was conducted in a parking lot. During both experiments, the whole-body antenna received station WWV at all four frequencies. Signal quality (indicated by the amount of static) was worse than the signal quality received by the 35-foot whip antenna, especially at a 5-MHz frequency. Signal quality at the 20-MHz frequency was very good.

When the whole-body antenna was used on a ground plane, reception quality degraded significantly when the shoes were disconnected from the rest of the circuit. Snapping the shoes back into the circuit reversed this degradation. No audible decline in reception quality from WWV was evident when the shoes were unsnapped in the parking lot. Capacitive coupling by the shoes eliminated the need to lengthen the antenna for reception in the parking lot.

INTEGRATION OF THREE ANTENNAS INTO ONE SYSTEM

The COMWIN antenna will be used with an ultra-wideband radio, the JTR. Thus, it is expected that there will be one output from the radio. The radio operator will select the frequency. Once the frequency is selected, all other issues such as signal route must be resolved. Because the COMWIN system has three antennas, this is an important issue.

A device such as a diplexer uses frequency and the impedance variation to change the signal path. The circuit is similar to a bandpass filter. The radio operator does not choose which antenna would transmit which signal. Such a procedure is good from the standpoint of automation but inadequate from the standpoint of device efficiency. A device such as a diplexer, which sends a signal along one of two paths depending on frequency, typically has high insertion loss. There must also be overlap between the frequency bands covered by each path of the diplexer. Thus, the diplexer-like solution is not the optimum one.

The ultra-wideband, handheld version of the JTR does not yet exist. This radio is expected to be ready for mass production by FY 2004. The radio, when it is produced, will likely have a two-bit, DC output signal that can activate the ports of a switch.

We decided that a switch is the optimum solution for the problem of the signal distribution to one of three antennas. Only one antenna at a time is expected to be active. There should be much isolation between signals in different paths. RF switches now on the market can provide 80 dB of isolation between paths. The downside is that until the architecture of the JTR is known, the radio operator must make a second decision and action concerning which antenna is the appropriate one for the signal (either transmit or receive) to use.

The COMWIN system has three antennas. When the vest antenna had a switch that optimized the matching in several bands, using another switch was difficult. There could be a return path not accounted for by the circuit. Fortunately, an average capacitor (56 pf) proved adequate for matching.

Searches of the literature by P.M. McGinnis indicated that the Narda[®] SEM133 SP3T switch could provide completely satisfactory performance characteristics. The advertised figures of merit were an insertion loss of 0.2 dB, isolation of 80 dB, and a VSWR of less than 1.2:1 in the 0.1- to 3000-MHz frequency range. The switch was activated by a 28-VDC signal that could be provided by three 9-V batteries in series. For ease of use, there must be a second switch that determined which port was opened. This switch, a simple DC version that can be hidden on the wrist, provided the control of the antenna to which the signal will be sent.

Figure 24 shows the Narda[®] SEM133 SP3T switch. The application of $28 \pm 3V$ on the appropriate terminal connected the input port to one of three ports. The length of the cylindrical part of the switch was 5 cm. The diameter was 3.5 cm. The length of the square base plate (used for screwing the switch into a bulkhead) was 4.5 cm. The switch had four SMA female connectors. The input was in the center. The other three were arranged in an equiangular manner. On the other end of the cylinder, the terminals for the DC voltage were arranged so that not only RF signals but also DC signals could be switched.



Figure 24. Narda[®] SEM133 SP3T switch to be used to channel signal from JTR to appropriate antenna in COMWIN system.

Figure 25 shows the VSWR from 5 to 1200 MHz for three cases. In the first case, the switch changed the path of the signal to go to the whole-body antenna. In the second case, the signal went to the vest antenna. In the third case, the signal went to the helmet antenna.

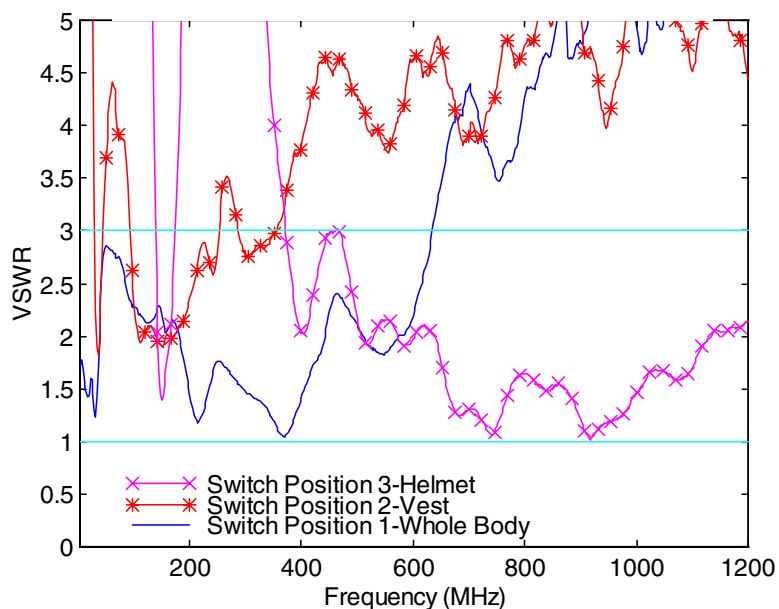


Figure 25. VSWR versus frequency of COMWIN antenna for three different modes of SP3T switch.

Figure 25 shows that in the 5- to 500-MHz frequency range, there is no frequency at which the VSWR is greater than 3:1 for all of the antennas in the COMWIN system.

RADIATION HAZARD MEASUREMENTS

The most important aspect of any antenna system is probably safety. This safety pertains to radiation hazards to the person's body, to ordnance, and to fuel. The fields to which the body is exposed must be below a certain number. This number depends upon frequency, volume of body exposed, and length of time of exposure. If only a small region of the body is exposed, the maximum field allowed is higher than if the whole body is exposed. Similarly, if the exposure is for a short time, the body can withstand much higher electric fields than long-term exposures. The Department of Defense, the Department of the Navy, and IEEE have all published similar standards for the maximum exposure of the whole body to electromagnetic fields (Department of Defense, 1995; Department of the Navy, 1995; Institute of Electrical and Electronics Engineers, 1991).

The thrust of most of the standards is to reduce the heating of the body. Phenomena such as cellular damage are expected to first manifest themselves as heat. A small volume of a healthy body exposed to an electromagnetic field will show a rise in temperature. Blood will then flow to that region to cool that part of the body. The rise in temperature should be proportional to the length of time to which the body is exposed. Most healthy human bodies can withstand a 1°C rise in temperature indefinitely. This rise is about what one would expect walking briskly on a warm day for about an hour.

The standards are quoted in terms of electric field strength (typically, 61.4 V/m over the whole body), or specific absorption rate (SAR), which is the amount of power absorbed per unit mass. The standards make a distinction between a controlled environment and an uncontrolled one. The assumption is that the people within the controlled environment know that there is a possible hazard. They can also take steps to reduce the hazard. People within an uncontrolled environment typically have no knowledge of any hazards. The standards for radiation exposure are correspondingly much stricter for an uncontrolled environment than for a controlled environment. We will use only the controlled environment standards.

ELECTRIC FIELD MEASUREMENTS IN EMPTY VEST ANTENNA

The electric fields within the vest antenna were measured as a function of frequency and location. The sensor used was the EMCO[®] E-field probe. Figure 26 shows this electric field sensor. This device was isotropic in that the electric field in all three perpendicular directions was summed as a vector. The result was a number that does not depend upon the orientation of the sensor. A coax cable connected the sensor to an interface unit. A fiber-optic cable connected the interface unit to the meter. The size of the sensor in figure 26 was 31-cm high. The sensitive part of the sensor was a cylinder 10 cm in diameter and approximately 10 cm in height. The probe was sensitive to electric fields as small as 0.5 V/m for frequencies between 1 and 1000 MHz.



Figure 26. EMCO[®] isotropic E-field sensor used for RADHAZ studies.

The signal generator and 50-dB power amplifier already described were used to energize the vest antenna in the 30- to 400-MHz frequency range. The power meter, spectrum analyzer, and bi-directional coupler already described measured and characterized the input power. We were careful to keep the input power constant at 5 W, independent of frequency. As a function of frequency, we calibrated the coupler and prepared a table of power values.

Figure 27 shows the results for the electric field as a function of frequency and location. The figure also shows the maximum permissible exposure (MPE) for a controlled environment. The major fields were confined to a region very close to the feed level. The fields decreased fairly rapidly as the sensor was raised or lowered. The probe was too large to determine any variation in the horizontal plane for the electric fields. The measurement site was a room in Building 377 in SSC San Diego. There were several large metal structures (cabinets and control panels) within 2 m of the observations. To make measurements of the fields outside the vest, the whole site was moved to the parking lot about 4 m from Building 377. The fiber-optic cable connected the sensor to the meter inside the building. The measurements showed that the field decreased monotonically as a function of distance. The field decreased to minimal values within 1 m of the vest.

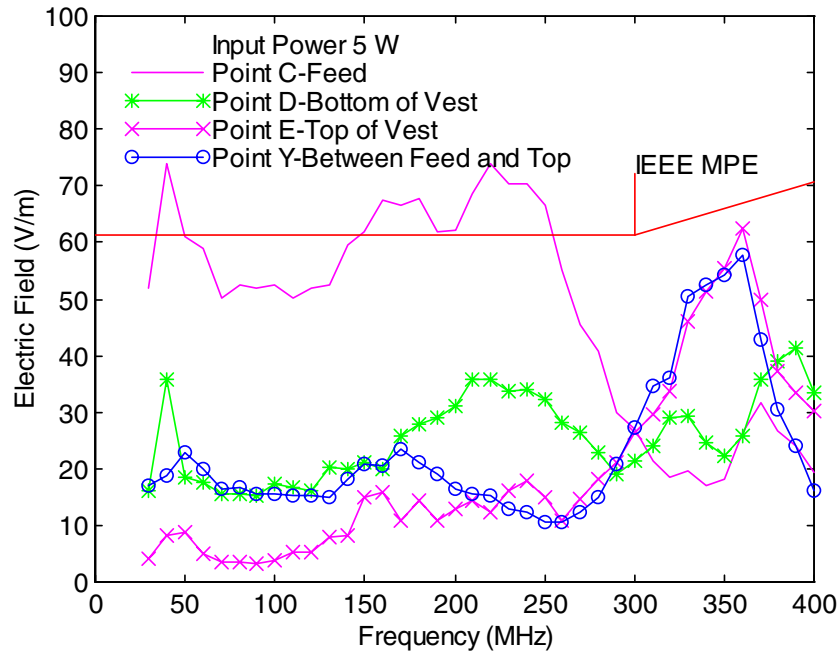


Figure 27. Electric fields within empty COMWIN vest antenna versus location and frequency.

The major reason for this measurement was to provide data for comparison of a finite difference time domain code that will be adapted and applied to the RADHAZ issue during FY 2002. The electric field very near the feed of the vest was also measured. The measurable quantity to which comparisons between theory and experiment will be made is the ratio of the field at a point to that at the feed. Using this quantity, we can minimize the input power or the amount of power returned to the transmitter because of mismatch.

There are three reasons why the measurements of the electric fields within the empty vest described above have only a marginal relevance. The first reason is that the sensor itself, although very sensitive, is also large. The field within the body is expected to vary with location, including horizontal position. Such a large sensor will average over this variation. The second reason is that the body will distort the fields very significantly. Even for the jell man to be described below in which the jell is homogeneous in composition, the shape of the body will lead to large variations in fields with respect to location. In particular, the body can focus the energy to a particular location. The third reason is that the antenna was designed for use with a person. The impedance of the antenna with a person inside is very different from the impedance with only the vest. The effect of the person is important to reduce mismatch losses. Without the person inside, there will be large mismatch losses and a corresponding decrease in the electric fields. Although measurement of the return power can be used to estimate the effective power input to the antenna, such a calculation is probably unrealistic.

MEASUREMENTS OF ELECTRIC FIELDS WITHIN THE BODY

On 10 through 12 July 2001, two researchers from SSC San Diego in association with researchers at the Naval Health Research Center (NHRC)–Detachment at Brooks AFB in San Antonio and Wayne Hammer of SPAWAR Systems Center, Charleston, conducted an experiment on the radiation

hazards of the vest and helmet antennas. SSC San Diego supplied the antennas, the signal generator, power meter, coupler, and amplifier. Brooks AFB supplied the sensors, three mannequins filled with jell to simulate a person in three frequency ranges, and the facility. The primary sensor was a pair of implantable E-field probes. Other sensors included a temperature sensor manufactured by Vitek® and an infrared sensor that measured temperature remotely. The most valuable quality supplied by the Brooks AFB and Wayne Hammer was expertise. Hammer and John D'andrea of NHRC are nationally known experts on the measurement, assessment, and mitigation of radiation hazards. The primary researcher who monitored the experiment was Dr. John Ziriak of the NHRC.

The sensor used was not calibrated for the low-frequency input. The vest antenna is needed at frequencies between 30 and 500 MHz. Unfortunately, the electric field sensor was calibrated at the factory only at 900 and 1800 MHz. Attempts to calibrate the sensor using measurements within a sphere have been unsuccessful. The tables below are the data measured by an uncalibrated sensor. Calibration at a frequency of 100 MHz shows that the implantable probe overestimates the electric field by 30%. Calibration has not been done at a 30-MHz frequency.

Figure 28 shows the sensor system with the interface unit. The NHRC had two of the units, a fact that reduced the time for measurements considerably. The probe was held in place by plastic restraints. Figures 29a and 29b show the probe with the cover assembled and with the cover removed. The probe was inserted into the jell man at 1 cm, 7.5 cm (near the center), and at 15 cm (about 1 cm from the edge). Care was needed on the choice of placement. The jell has the consistency of oatmeal. If the probe were removed, an air gap would occur. This would invalidate the measurements. An hour's wait was required so that the gap would refill.

- Multiplexed three-channel single-ended inputs
- 16-bit A-to-D converter w/programmable gain
- Optical link to RS-232 connector
- Two readings per second
- Factory calibrated at 1800 and 900 MHz



Figure 28. Implantable E-field probe from SARTest LTD.

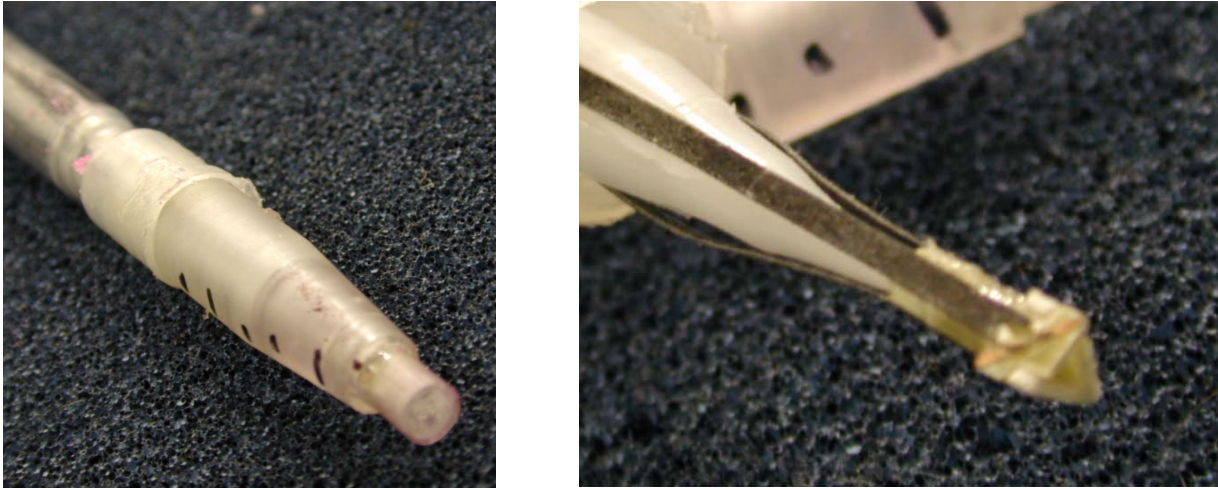


Figure 29. Probe with cover assembled (left) and with cover removed (right).

Figure 30 shows the mannequin filled with jell. The locations of the eight measurement sites are also indicated. The distance between sites was approximately 10 cm. The probe was inserted down to three depths at each measurement site. The mannequin was placed on a wooden table in the NHRC Anechoic Chamber. The original plan was to place the mannequin on top of the feed. Numerous measurements were obtained. The electric fields measured were all smaller than the maximum permissible exposure, even for an input of 50 W. Suspicions were raised when the measurement of the impedance and VSWR showed that the reflected power was very large. There was a severe mismatch because of the distortion of the feed by the weight of the mannequin.

This mismatch was overcome by putting the vest antenna feed on top of the mannequin. Measurements were taken of the VSWR of the vest antenna on the mannequin and on several of the researchers. Figure 31 shows this comparison for the 30- to 100-MHz range. After this experience, a careful watch was made of the returned power as measured from the power meter attached to the second port of the bi-directional coupler. The returned power was subtracted from the input to give the effective power used by the antenna either to send energy to infinity (good) or to heat the jell man (bad).

- Test vest front side down
- Eight locations
 - 10 cm lateral
 - mid-gap (2)
 - mid-conductor (4)
 - 2 cm above & below (2)
- Three depths @ each location
 - 1 cm deep
 - Center
 - 1 cm from back



Figure 30. Mannequin filled with jell.

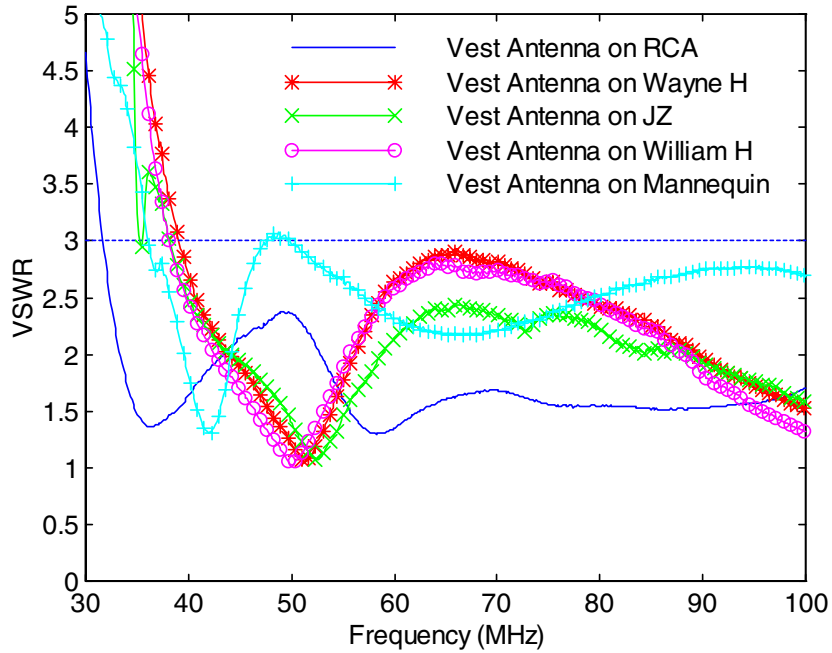


Figure 31. Comparison of VSWR versus frequency of vest antenna on mannequin and on various researchers in 30- to 100-MHz range.

Figure 32 presents a similar comparison for the VSWR of the vest antenna versus frequency when worn by RCA and by the mannequin in the 100- to 500-MHz range. In this frequency range, the comparison is even better.

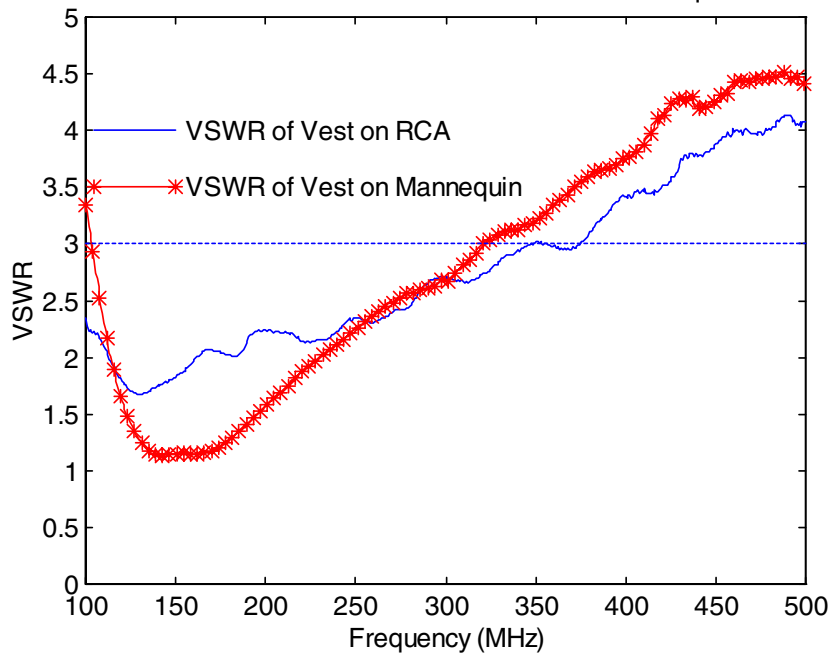


Figure 32. Comparison of VSWR versus frequency of vest antenna when worn by mannequin and by person in 100- to 500-MHz range.

Table 5 presents the composition of the jell man by weight. For frequencies above 100 MHz, the constituents of the jell were a petroleum product, TX-150 to solidify the jell, polyethylene powder, water, and salt to provide conductivity. Below 100 MHz, aluminum powder was used. Together, the ingredients added up to approximately 70 kg. Chou et al. (1984) described the experiments that provided the recipe for the jell used in various frequency ranges. Three jell men were fabricated. A sphere was also filled with the jell for the 300- to 915-MHz frequency range so that the radiation hazards of the helmet could be assessed.

Table 5. Composition by weight of jell man for various frequency ranges.

Frequency (MHz)	TX-150 (kg)	Polyethylene Powder (kg)	Aluminum Powder (kg)	Water (kg)	Salt (kg)	Total Weight (kg)
40.68	6.776	0	6.44	56.574	0.212	70.002
200	5.873	11.053	0	52.444	0.626	69.996
300 to 915	5.894	10.808	0	52.605	0.697	70.004

Table 6 presents the data from the uncalibrated electric field probes for when the probe was very near the surface. This was the worst case. The sites near the feed had the largest fields. The jell composition used was that for 40.68 MHz. The column labeled PM was the reading from the power meter. Because nearly 50 W (47 dBm) was being input, the coupler sometimes did not provide enough attenuation. A 6-dB attenuation was inserted on one port of the coupler. The return power was also measured. The total effective power was that input to the antenna. This input was calculated by using the measured relationship between input to port readings of the coupler and the difference between input and return power. This result was the power that actually went to the antenna. All the tables are labeled the same. The data for the total effective power for a given frequency was assumed to be independent of the location of the probes. This assumption was explicitly checked for the case of the helmet and found valid to within 1 dB.

Tables 6 through 14 list the x, y, z coordinates of the probe. The coordinates were measured relative to the x-y location of the feed and the center of the mannequin.

Table 6. Electric field data for 41-MHz composition and depth of probe 1 cm into back of mannequin.

Height z=7.5 cm	PM		Total	x (cm)		y (cm)		x (cm)		y (cm)		x (cm)		y (cm)	
	0	-6		6	-6	6	-6	6	-8.77	-8.77	-8.77	6	6	-18.77	6
	18.77	8.77	8.77	0	0	0	0	0	0	0	0	0	0	0	0
	91.7	390.5	738.0	28.5	10.0	89.1	117.4	3.2	3.7	3.7	3.7	3.7	3.7	3.7	3.7
30	4.63	6.8	29.37	127.0	515.5	912.0	47.7	13.9	102.1	137.9	137.9	137.9	137.9	137.9	137.9
35	5.84	7.31	32.46	113.6	468.8	880.0	32.2	11.5	101.8	142.5	142.5	142.5	142.5	142.5	142.5
40	7.05	7.68	35.57	116.7	484.1	920.8	41.2	12.6	96.1	137.5	137.5	137.5	137.5	137.5	137.5
45	7.95	5.12	43.55	106.7	441.1	896.8	43.5	12.6	81.7	117.7	117.7	117.7	117.7	117.7	117.7
50	8.84	3.36	46.56	87.6	369.2	765.6	43.6	12.1	58.4	88.5	88.5	88.5	88.5	88.5	88.5
55	9.54	2.5	47.63	64.4	288.9	646.0	26.3	9.6	47.9	74.5	74.5	74.5	74.5	74.5	74.5
60	10.23	3.99	47.13	49.5	222.5	532.4	17.7	8.4	37.3	58.1	58.1	58.1	58.1	58.1	58.1
65	10.83	4.74	47.02	43.1	183.3	444.8	14.8	8.5	30.0	49.1	49.1	49.1	49.1	49.1	49.1
70	11.42	4.34	47.66	38.5	153.5	401.2	12.8	8.1	24.8	41.5	41.5	41.5	41.5	41.5	41.5
75	11.95	5.51	47.26	35.0	135.4	356.0	12.2	8.9	21.5	37.4	37.4	37.4	37.4	37.4	37.4
80	12.47	8.56	45.01	28.1	110.2	298.8	13.4	9.9	17.0	30.6	30.6	30.6	30.6	30.6	30.6
85	12.92	9.63	44.22	21.6	87.0	246.8	14.8	10.4	12.9	24.5	24.5	24.5	24.5	24.5	24.5
90	13.37	9.63	44.80	7.8	38.5	78.0	20.5	12.4	5.2	8.7	8.7	8.7	8.7	8.7	8.7
120	14.80	11.04	37.15	7.5	36.4	74.0	19.6	11.7	4.9	7.4	7.4	7.4	7.4	7.4	7.4
130	16.22	12.98	44.15	7.2	33.2	84.8	17.4	11.0	4.8	6.5	6.5	6.5	6.5	6.5	6.5
140	16.74	13.52	43.92	6.6	29.9	122.4	15.1	9.9	4.4	6.0	6.0	6.0	6.0	6.0	6.0
150	17.26	13.97	44.22												

Table 7 presents the electric fields measured in the 41-MHz composition when the probe was inserted 7.5 cm. When the probe was near the center, the fields were very small. A reading of 0.0 implies that the measurement was taken, but the reading was below the 1.5-V/m sensitivity level of the probe.

Table 7. Electric field data for 41-MHz composition and depth of probe near center of mannequin.

Height z=0 cm	PM 6-dB Attenuation (dBm)		Return Power (dBm)	Total Effective Power (W)	E V/m											
	x (cm)	y (cm)			x (cm)	y (cm)										
	0	-6			18.77	8.77	8.77	0	0	0	6	-6	6	-6	6	-18.77
30	4.63	6.8	29.37	0.0	18.9	12.1	0.0	2.8	7.5	8.0	3.1	7.5	8.0	3.1	7.5	8.0
35	5.84	7.31	32.46	0.0	20.6	12.9	0.0	3.2	8.1	8.3	3.7	8.1	8.3	3.7	8.1	8.3
40	7.05	7.68	35.57	0.0	17.2	9.6	0.0	3.1	7.0	7.6	3.5	7.0	7.6	3.5	7.0	7.6
45	7.95	5.12	43.55	0.0	15.2	7.9	1.3	3.3	6.8	7.0	3.7	6.8	7.0	3.7	6.8	7.0
50	8.84	3.36	46.56	0.0	12.1	5.8	1.0	3.5	5.9	5.8	4.2	5.9	5.8	4.2	5.9	5.8
55	9.54	2.5	47.63	0.0	8.5	2.7	0.0	3.5	5.3	4.6	3.9	5.3	4.6	3.9	5.3	4.6
60	10.23	3.99	47.13	0.0	5.4	0.0	0.0	3.4	4.3	4.0	3.6	4.3	4.0	3.6	4.3	4.0
65	10.83	4.74	47.02	0.0	2.9	0.0	0.0	3.2	4.1	3.7	3.6	4.1	3.7	3.6	4.1	3.7
70	11.42	4.34	47.66	0.0	1.2	0.0	0.0	2.9	4.0	3.7	2.6	4.0	3.7	2.6	4.0	3.7
75	11.95	5.51	47.26	0.0	0.0	0.0	0.0	3.0	3.8	3.2	2.6	3.8	3.2	2.6	3.8	3.2
80	12.47	8.56	45.01	0.0	1.5	0.0	0.0	3.0	3.5	3.0	2.8	3.5	3.0	2.8	3.5	3.0
85	12.92	9.63	44.22	0.0	0.0	0.0	0.0	3.0	3.0	3.1	2.6	3.0	3.1	2.6	3.0	3.1
90	13.37	9.63	44.80	0.0	0.0	0.0	0.0	3.0	2.3	3.3	2.1	2.3	3.3	2.1	2.3	3.3
120	14.80	11.04	37.15	0.0	0.0	0.0	0.0	2.7	1.7	3.0	1.5	1.7	3.0	1.5	1.7	3.0
130	16.22	12.98	44.15	0.0	0.0	0.0	0.0	2.7	2.2	2.3	2.0	2.2	2.3	2.0	2.2	2.3
140	16.74	13.52	43.92	0.0	0.0	0.0	0.0	2.7	2.3	2.2	2.2	2.3	2.2	2.2	2.3	2.2
150	17.26	13.97	44.22	0.0	0.0	0.0	0.0	2.7	2.4	2.2	2.0	2.4	2.2	2.0	2.4	2.2

Table 8 shows the electric field measurements for the case of the jell composition for 40.68 MHz when the probe was approximately 1 cm from the edge near the front of the vest. This was often an intermediate case between the location near the feed on the back and those near the center.

Table 8. Electric field data for 41-MHz composition and depth of probe near front of mannequin.

Freq. (MHz)	PM 6-dB Attenuation (dBm)	Return Power (dBm)	Effective Power (W)	Total		l3		m3		n3		o3		p3		q3		r3		s3			
				x (cm)	y (cm)																		
z = - 7.5 cm																							
				18.77	0	8.77	-6	8.77	6	8.77	6	0	-6	0	6	0	-6	-8.77	-6	-8.77	6	-18.77	6
30	4.63	6.8	29.37	0.0	0.0	12.2	18.8	10.5	16.1	13.4	15.9	10.3	12.3	5.7									
35	5.84	7.31	32.46	0.0	0.0	18.8	22.1	18.8	23.6	27.6	23.4	14.4	17.7	8.1									
40	7.05	7.68	35.57	3.1	3.1	25.7	22.0	22.0	27.6	32.5	27.6	16.4	20.9	8.6									
45	7.95	5.12	43.55	3.8	3.8	26.2	23.1	29.0	35.0	35.0	35.0	18.9	24.2	10.4									
50	8.84	3.36	46.56	3.2	3.2	22.8	22.0	26.6	32.9	32.9	32.9	19.6	25.9	11.3									
55	9.54	2.5	47.63	0.0	0.0	20.9	20.1	25.5	32.3	32.3	32.3	17.9	23.1	10.5									
60	10.23	3.99	47.13	0.0	0.0	20.2	19.0	24.6	31.3	31.3	31.3	15.8	21.7	9.2									
65	10.83	4.74	47.02	0.0	0.0	21.0	19.0	24.9	31.4	31.4	31.4	14.6	20.4	8.2									
70	11.42	4.34	47.66	0.0	0.0	21.9	19.7	26.0	33.0	33.0	33.0	14.4	20.0	6.9									
75	11.95	5.51	47.26	0.0	0.0	24.3	21.5	27.9	35.3	35.3	35.3	13.1	21.0	8.2									
80	12.47	8.56	45.01	0.0	0.0	24.1	21.1	27.6	35.4	35.4	35.4	15.0	22.9	9.2									
85	12.92	9.63	44.22	0.0	0.0	22.9	19.8	26.3	34.2	34.2	34.2	14.8	22.8	8.4									
90	13.37	9.63	44.80	0.0	0.0	19.1	14.3	19.9	29.9	29.9	29.9	13.6	21.8	7.8									
120	14.80	11.04	37.15	0.0	0.0	19.6	12.4	20.3	26.4	26.4	26.4	10.9	19.3	5.9									
130	16.22	12.98	44.15	0.0	0.0	20.5	11.4	19.0	24.7	24.7	24.7	10.6	18.3	5.6									
140	16.74	13.52	43.92	0.0	0.0	19.8	10.1	10.1	15.7	15.7	15.7	10.4	17.0	4.7									
150	17.26	13.97	44.22	0.0	0.0									4.2									

Table 9 presents the electric field data for using the composition of the jell man for 200 MHz. The locations of the probes were the same. The depth of the probe was 1 cm from the back.

Table 9. Electric field data for 200-MHz composition and depth of probe 1 cm into back of mannequin.

z = 7.5 cm	0		-6		6		-6		6		-6		6		-18.77	
	x(cm) y(cm)	E V/m														
150	17.26	-0.97	49.93	13.4	34.9	783.69	35.40	58.6	34.5	18.9	6.3	17.26	-0.97	49.93	13.4	34.9
160	17.73	-0.68	49.94	11.6	34.4	694.00	40.53	54.8	38.3	22.8	6.6	17.73	-0.68	49.94	11.6	34.4
170	18.16	3.61	49.68	10.2	35.9	603.97	45.09	53.2	41.8	26.3	6.4	18.16	3.61	49.68	10.2	35.9
180	18.54	4.38	49.64	9.3	37.7	524.18	48.18	52.2	44.5	28.9	7.3	18.54	4.38	49.64	9.3	37.7
190	18.89	8.29	49.03	8.6	38.5	447.27	48.71	51.9	45.2	29.8	9.5	18.89	8.29	49.03	8.6	38.5
200	19.21	10.56	48.40	9.0	39.3	394.58	48.97	51.7	45.6	30.4	11.5	19.21	10.56	48.40	9.0	39.3
210	19.51	11.72	48.03	8.9	38.9	353.45	48.18	52.0	45.4	30.4	11.3	19.51	11.72	48.03	8.9	38.9
220	19.78	13.94	46.84	8.7	37.5	319.71	47.07	52.1	45.2	30.1	10.5	19.78	13.94	46.84	8.7	37.5
230	20.04	14.19	46.85	9.1	36.5	305.65	46.81	54.2	47.1	31.1	10.0	20.04	14.19	46.85	9.1	36.5
240	20.26	15.96	45.44	8.7	33.0	258.11	44.24	52.1	45.6	29.9	9.6	20.26	15.96	45.44	8.7	33.0
250	20.46	16.28	45.31	9.2	31.5	233.18	43.87	52.6	46.7	30.2	9.7	20.46	16.28	45.31	9.2	31.5
260	20.65	17.48	44.05	9.2	29.1	199.29	41.31	50.0	45.4	29.0	9.1	20.65	17.48	44.05	9.2	29.1
270	20.82	17.77	43.88	9.7	28.9	179.45	40.79	49.1	46.1	29.0	9.2	20.82	17.77	43.88	9.7	28.9
280	20.97	19.37	41.41	11.7	28.5	159.57	38.76	46.8	44.9	32.8	9.0	20.97	19.37	41.41	11.7	28.5
290	21.11	18.47	43.27	9.8	28.8	147.21	38.42	45.2	44.8	28.2	8.8	21.11	18.47	43.27	9.8	28.8
300	21.20	18.55	43.28	9.2	28.8	136.34	37.42	43.6	44.8	27.9	8.2	21.20	18.55	43.28	9.2	28.8

Table 10 presents the electric field data for using the composition of the jell man for 200 MHz. The locations of the probes were the same as that described in figure 30. The depth of the probe was at the center of the mannequin.

Table 10. Electric field data for 200-MHz composition and depth of probe at center of mannequin.

z = 0 cm	PM		Total Effective Power (W)	E		E		E		E		E		E	
	6-dB Attenuation (dBm)	Return Power (dBm)		x(cm)	y(cm)										
150	17.26	-0.97	49.93	12.6	18.9	17.3	7.7	11.8	11.2	15.1	7.3				
160	17.73	-0.68	49.94	11.2	16.9	15.2	7.9	12.2	10.8	14.2	6.1				
170	18.16	3.61	49.68	10.2	14.8	13.2	10.4	13.2	10.9	13.2	5.2				
180	18.54	4.38	49.64	9.2	13.5	12.0	13.0	14.4	11.7	12.1	4.3				
190	18.89	8.29	49.03	8.0	12.6	10.7	14.5	14.8	12.3	11.3	4.1				
200	19.21	10.56	48.40	7.4	12.8	10.3	15.5	15.1	12.8	11.1	4.1				
210	19.51	11.72	48.03	5.8	12.7	10.1	15.8	15.2	12.9	10.9	4.1				
220	19.78	13.94	46.84	3.9	12.4	10.3	15.7	15.2	12.6	10.7	4.0				
230	20.04	14.19	46.85	1.7	13.1	11.4	15.8	16.6	12.9	10.7	4.2				
240	20.26	15.96	45.44	0.0	11.3	11.7	14.8	15.3	12.0	10.2	3.4				
250	20.46	16.28	45.31	0.0	10.9	12.5	14.6	15.7	12.0	9.9	3.0				
260	20.65	17.48	44.05	0.0	10.0	12.6	13.8	15.0	11.5	9.1	2.4				
270	20.82	17.77	43.88	0.0	9.9	12.9	13.6	14.8	11.5	8.8	2.3				
280	20.97	19.37	41.41	0.0	9.9	12.8	13.0	14.1	11.1	8.4	2.3				
290	21.11	18.47	43.27	0.0	10.1	12.6	12.8	13.7	11.0	8.1	2.3				
300	21.20	18.55	43.28	0.0	10.1	12.0	12.5	13.0	10.9	7.0	2.0				

Table 11 shows the electric field data for using the composition of the jell man for 200 MHz. The locations of the probes were the same as those described in figure 30. The depth of the probe was 1 cm from the front of the mannequin.

Table 11. Electric field data for 200-MHz composition and depth of probe 1 cm into front of mannequin.

z = -7.5 cm		0		-6		6		-6		6		-6		6	
PM	6-dB Attenuation (dBm)	Return Power (dBm)	Total Effective Power (W)	x(cm) y(cm)											
150	17.26	-0.97	49.93	0.0	33.5	37.8	33.7	36.2	36.7	35.6	22.3	17.26	-0.97	49.93	0.0
160	17.73	-0.68	49.94	0.0	32.7	36.0	31.9	32.6	36.5	32.2	21.4	17.73	-0.68	49.94	0.0
170	18.16	3.61	49.68	0.0	30.3	33.2	28.7	28.1	33.8	28.4	19.6	18.16	3.61	49.68	0.0
180	18.54	4.38	49.64	0.0	27.1	29.3	24.4	22.9	30.0	24.4	17.2	18.54	4.38	49.64	0.0
190	18.89	8.29	49.03	4.2	23.9	24.9	19.7	18.3	25.7	20.6	14.4	18.89	8.29	49.03	4.2
200	19.21	10.56	48.40	8.1	22.8	21.8	16.1	15.9	23.1	18.7	12.7	19.21	10.56	48.40	8.1
210	19.51	11.72	48.03	8.3	21.2	19.3	13.5	14.9	21.8	17.9	11.9	19.51	11.72	48.03	8.3
220	19.78	13.94	46.84	7.7	19.9	17.1	12.2	14.3	20.8	17.8	11.2	19.78	13.94	46.84	7.7
230	20.04	14.19	46.85	6.6	19.4	15.4	11.7	13.8	20.3	18.1	10.3	20.04	14.19	46.85	6.6
240	20.26	15.96	45.44	5.4	18.0	13.7	11.3	12.8	19.3	17.9	10.2	20.26	15.96	45.44	5.4
250	20.46	16.28	45.31	4.7	17.5	12.6	11.4	11.9	19.2	18.1	10.0	20.46	16.28	45.31	4.7
260	20.65	17.48	44.05	3.0	16.0	11.3	11.0	10.1	18.4	17.3	9.3	20.65	17.48	44.05	3.0
270	20.82	17.77	43.88	2.9	15.7	10.7	11.0	8.8	18.5	17.1	9.2	20.82	17.77	43.88	2.9
280	20.97	19.37	41.41	3.7	15.8	10.2	11.1	7.7	18.4	16.8	8.8	20.97	19.37	41.41	3.7
290	21.11	18.47	43.27	4.0	16.1	10.5	11.4	7.2	18.6	16.8	8.6	21.11	18.47	43.27	4.0
300	21.20	18.55	43.28	3.8	16.3	10.7	11.5	6.6	18.7	16.6	8.4	21.20	18.55	43.28	3.8

Table 12 presents the electric field data for using the composition of the jell man for the highest frequencies. The locations of the probes were the same as those described in figure 30. The depth of the probe was 1 cm from the back.

		0		-6		6		-6		6		-6		6		-18.77	
		x(cm)	y(cm)	x(cm)	y(cm)	x(cm)	y(cm)	x(cm)	y(cm)	x(cm)	y(cm)	x(cm)	y(cm)	x(cm)	y(cm)	x(cm)	y(cm)
z = 7.5 cm		E V/m		E V/m		E V/m		E V/m		E V/m		E V/m		E V/m		E V/m	
PM 6 dB attenuation dBm	Return Power (dBm)	Total Effective Power (W)															
Freq. (MHz)			I1	m1	n1	o1	p1	q1	r1	s1							
300	21.20	18.64	43.14	9.7	48.3	39.8	49.1	49.7	44.5	38.3	8.6						
310	21.31	19.17	42.43	9.2	44.4	39.5	47.5	48.3	43.6	37.8	8.4						
320	21.39	19.08	42.73	8.6	42.0	39.9	47.6	48.2	43.9	37.9	8.1						
330	21.49	19.89	41.41	7.6	38.1	38.3	45.5	45.7	42.2	36.5	7.7						
340	21.55	19.69	41.92	7.0	37.9	38.9	46.7	46.3	43.4	37.1	7.7						
350	21.58	20.16	41.04	5.9	37.1	37.8	45.6	45.3	42.5	35.7	7.4						
360	21.62	20.15	41.15	5.6	36.5	36.9	45.1	44.1	42.0	35.8	7.3						
370	21.63	20.47	40.48	5.0	35.7	35.0	43.3	42.1	40.4	34.5	6.9						
380	21.63	20.59	40.21	4.5	35.8	34.2	42.6	41.3	39.8	33.8	6.8						
390	17.80	17.02	16.40	2.9	22.3	21.1	26.0	25.6	34.4	20.5	4.3						
400	21.61	20.7	39.91	4.0	34.8	32.3	39.3	39.1	37.3	31.5	6.6						

Table 13 presents the electric field data for using the composition of the jell man for the highest frequencies. The locations of the probes were the same as those described in figure 30. The depth of the probe was at the center.

Table 13. Electric field data for 300-MHz composition and depth of probe at center of mannequin.

z = 0 cm	PM	6-dB Attenuation (dBm)	Return Power (dBm)	Total Effective Power (W)	E		E		E		E		E	
					x(cm) y(cm)	x(cm) y(cm)	x(cm) y(cm)	x(cm) y(cm)	x(cm) y(cm)	x(cm) y(cm)				
300	21.20	18.64	43.14	0.0	18.77	8.77	8.77	8.77	0	0	0	-8.77	-8.77	-18.77
310	21.31	19.17	42.43	0.0	15.7	15.7	11.8	10.2	16.4	16.4	11.7	10.5	4.1	
320	21.39	19.08	42.73	0.0	15.2	15.2	11.8	10.0	16.4	16.4	11.8	10.5	4.2	
330	21.49	19.89	41.41	0.0	13.8	13.8	11.1	9.3	15.6	15.6	11.5	10.0	4.0	
340	21.55	19.69	41.92	0.0	13.7	13.7	11.3	9.5	15.7	15.7	11.8	10.1	4.0	
350	21.58	20.16	41.04	0.0	12.9	12.9	10.6	10.4	14.9	14.9	11.4	10.0	3.3	
360	21.62	20.15	41.15	0.0	12.4	12.4	10.1	8.9	14.8	14.8	11.5	9.7	3.7	
370	21.63	20.47	40.48	0.0	11.6	11.6	9.4	8.3	14.0	14.0	10.9	9.3	3.4	
380	21.63	20.59	40.21	0.0	11.1	11.1	9.0	8.1	13.7	13.7	10.8	9.1	3.3	
390	17.80	17.02	16.40	0.0	5.4	5.4	3.8	3.2	8.4	8.4	6.6	5.6	1.8	
400	21.61	20.7	39.91	0.0	9.2	9.2	7.8	6.7	12.8	12.8	10.0	8.6	2.9	

Table 14 presents the electric field data for using the composition of the jell man for the highest frequencies. The locations of the probes were the same as those described in figure 30. The depth of the probe was 1 cm from the front.

Table 14. Electric field data for 300-MHz composition and depth of probe 1 cm into front of mannequin.

z = -7.5 cm		x(cm)		y(cm)		x(cm)		y(cm)		x(cm)		y(cm)		x(cm)		y(cm)	
0	-6	6	-6	0	6	-6	0	6	-6	6	-6	6	-6	6	-6	6	-6
PM	6-dB	Return	Total	E	E	E	E	E	E	E	E	E	E	E	E	E	E
Attenuation	Power	Power	Effective	V/m	V/m	V/m	V/m	V/m	V/m	V/m	V/m	V/m	V/m	V/m	V/m	V/m	V/m
(MHz)	(dBm)	(dBm)	(W)	I3	m3	n3	o3	p3	q3	r3	s3						
300	21.20	18.64	43.14	0.0	14.5	16.1	2.2	13.1	8.2	12.5	14.8						
310	21.31	19.17	42.43	0.0	14.0	15.1	2.5	12.5	7.6	12.0	14.4						
320	21.39	19.08	42.73	0.0	13.7	14.4	3.0	12.1	7.4	11.7	14.3						
330	21.49	19.89	41.41	0.0	12.4	12.6	2.9	10.9	6.9	10.9	13.3						
340	21.55	19.69	41.92	0.0	11.8	11.8	3.3	10.5	6.9	10.8	13.0						
350	21.58	20.16	41.04	0.0	10.0	9.7	2.4	9.1	6.4	9.8	11.7						
360	21.62	20.15	41.15	0.0	9.1	9.1	2.9	8.8	6.3	9.4	11.5						
370	21.63	20.47	40.48	0.0	7.5	7.9	2.6	8.1	5.9	8.6	10.6						
380	21.63	20.59	40.21	0.0	6.3	7.3	2.6	8.0	5.9	8.2	10.0						
390	17.80	17.02	16.40	0.0	0.0	1.8	0.0	4.9	3.6	4.8	5.9						
400	21.61	20.7	39.91	0.0	3.6	6.6	0.0	7.9	5.9	7.3	8.9						

Figures 33 and 34 shows the specific absorption rate data for the two worst locations (labeled as M and N) on the figures. The specific absorption rate (in W/kg) is the primary measure of how much power is absorbed into the body as heat. A total of 4 W/kg is the maximum permitted for a body. The total can go as high as a factor of 5 larger for a 1-g cube.

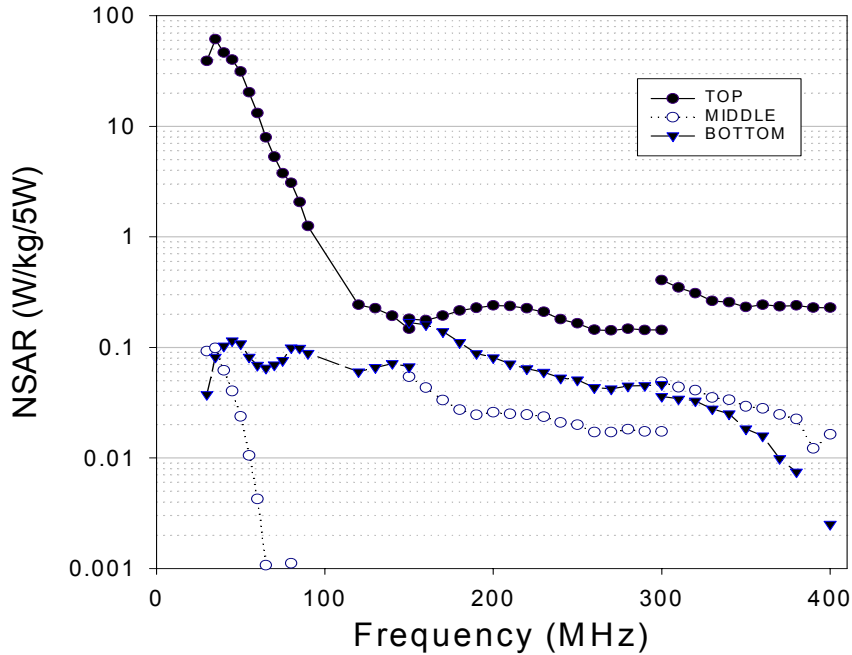


Figure 33. Specific absorption rate in W/kg for vest antenna versus frequency for three different compositions of jell and three different depths of probe for Site M.

Site M was located above and just to the left of the feed. Three different compositions of jell were used in the frequency ranges 30 to 150 MHz, 150 to 300 MHz, and 300 to 400 MHz. Figure 33 provides data for three different depths of the probe. These are near the surface at the back, at the center of the mannequin, and near the surface at the front. The worst points from a radiation hazard were located near the back where the feed is located.

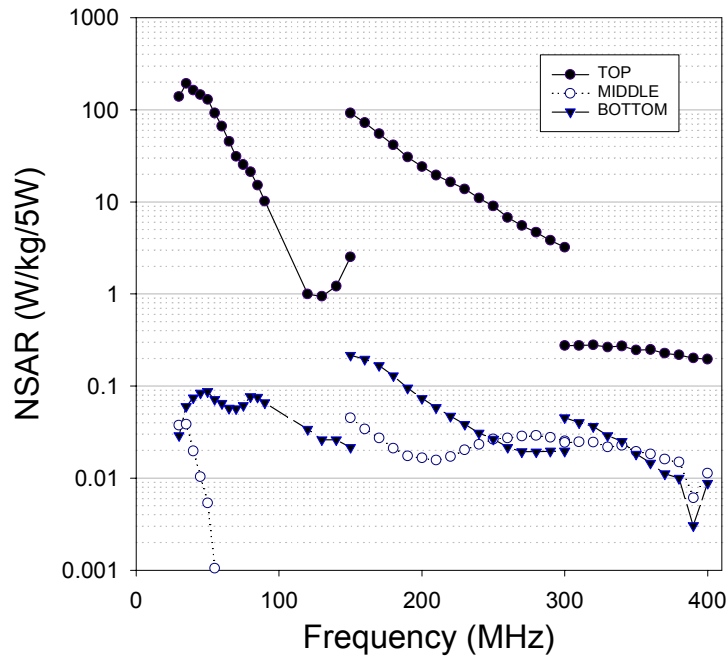


Figure 34. Specific absorption rate in W/kg for vest antenna versus frequency for three different compositions of jell and three different depths of probe for Site N.

Site N was located above and just to the right of the feed.

Similar observations were made of the radiation hazards for the helmet antenna. The amplifier could go to a frequency only of 1000 MHz. Figure 35 shows the experimental arrangement of the probes in the helmet. The measurement sites were in the center of the head, near the feed, and near the top of the helmet (corresponding to the bottom of the photograph).

- 1 cm from inside top of phantom
- 1 cm in at point closest to feed
- Center of sphere

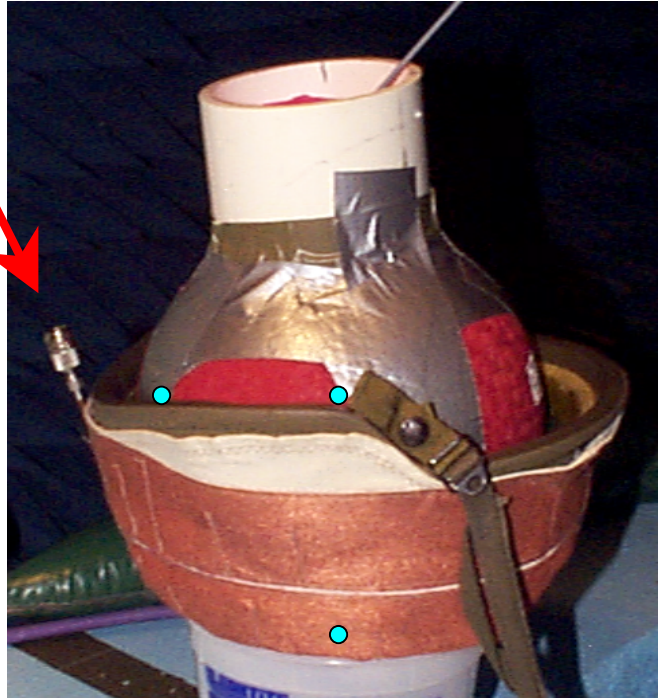


Figure 35. Experimental arrangement for measurement of electric fields within helmet antenna.

The VSWR versus frequency of the helmet antenna on the mannequin was also measured and compared with that of a person. Figure 36 shows this comparison. The Anritsu[®] Sitemaster measured the VSWR for the mannequin from 400 to 1000 MHz. The Hewlett Packard[®] HP8510C network analyzer measured similar data for the helmet on a person.

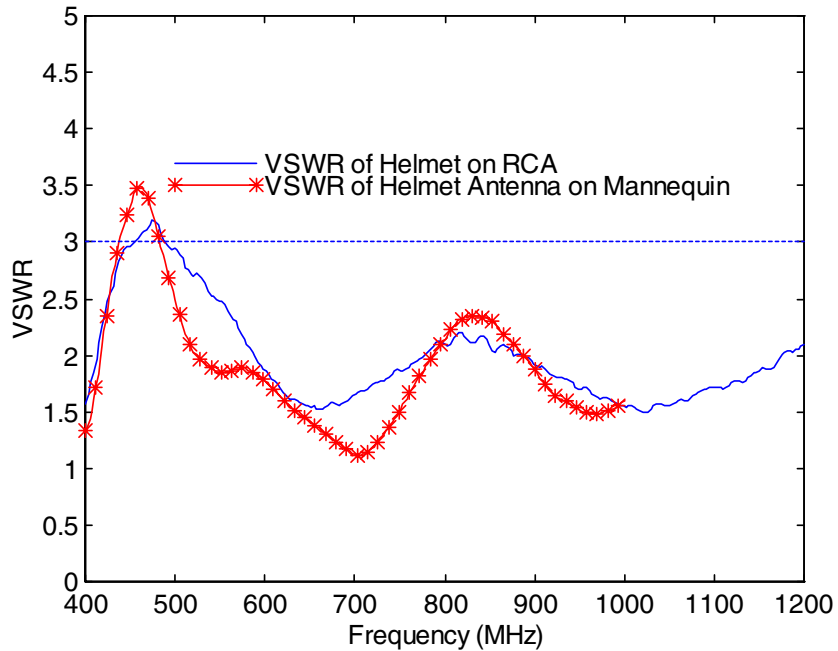


Figure 36. VSWR versus frequency of helmet antenna on a mannequin and on a person.

The comparison between the data on the COMWIN vest or helmet antennas on the person and on the mannequins showed fairly clearly that the dielectric and conductive properties were similar. Table 15 shows the data for the electric fields measured at the three locations in the helmet antenna as a function of location. The column heads have the same meaning as in the previous tables. The return power was measured for each probe location. There was little difference due to the probe. The data showed that even at an input power of 50 W, the maximum permissible exposure levels were not exceeded.

Table 15. Electric fields measured within jell man when 50 W of power are input to helmet antenna.

(MHz) Freq. (MHz)	PM 6-dB Attenuation	Return Power Feed (dBm)	Total		Return Power Center (dBm)	Total		E V/m Feed	E V/m Center	E V/m Top
			Effective Power Feed (W)	Return Power Center (dBm)		Effective Power Center (W)	Return Power Top (dBm)			
400	19.66	12.20	30.54	12.22	30.54	13.54	30.03	22.6	22.8	41.5
450	18.50	16.59	20.86	16.54	20.86	16.33	21.05	28.0	15.3	22.5
500	20.00	14.65	35.38	14.00	35.38	13.79	35.49	45.8	19.8	16.9
550	20.00	11.90	38.39	12.04	38.39	11.73	38.50	43.9	18.6	14.9
600	20.00	12.16	41.71	12.03	41.71	12.02	41.72	37.4	16.4	13.3
650	20.00	10.64	42.68	9.92	42.68	9.77	42.71	28.6	16.4	12.5
700	20.00	1.40	41.53	-1.90	41.53	-2.08	41.53	25.9	14.8	11.2
750	20.00	7.80	37.58	9.60	37.58	9.31	37.64	26.7	12.2	11.0
800	20.00	14.64	33.03	14.66	33.03	14.42	33.17	23.0	9.9	9.8
850	20.00	15.04	31.58	14.47	31.58	14.11	31.77	18.6	8.4	9.0
900	20.00	12.14	32.88	10.73	32.88	10.21	32.99	20.2	6.5	9.5
950	20.00	4.96	35.80	4.64	35.80	4.10	35.83	24.7	5.0	9.2
1000	19.00	7.56	32.66	8.60	32.66	8.57	32.66	25.0	5.3	7.4

The data from the probes indicated a radiation hazard problem in the vest antenna. The infrared camera showed that the rise in temperature over a period of hours (50 W being input to the mannequin on a continuous basis) was as much as 15°C. The body actually became hot to the touch.

The problem was indicative of the solution. The fields within the mannequin were small. These fields were excluded by the conductivity of the body. The fields acted to heat up the surface, which then heated up the rest of the body. Shielding of the body by some of the FlecTron[®] material is one solution. Unfortunately, this would probably lead to a great reduction in antenna bandwidth.

The solution is to use a material that is lightly conductive (1 S/m) near the feed to absorb some of the energy and keep it from the body. This material might get hot. Shielding the human from heat is straightforward. The material in question could be the material used in the jell man. This material, as shown by the VSWR data, clearly retains the broadband nature of the antenna. The material also shields the interior of the body from RF energy. The use of aluminum powder should be minimized. Salt water solidified by TX-150 seems to be a solution to the problem. This material can be mixed and will remain good for weeks. The resulting mixture has the consistency of oatmeal. Nonetheless, this material, if used in an airtight bag, could shield the person from the energy radiated by the vest antenna.

There is undoubtedly an optimum solution. A Joule of energy that goes to heat up material is a Joule that is wasted. Ideally, the energy should be reflected rather than absorbed. Research must be done to find this optimum solution.

CONCLUSIONS

The vest antenna is the primary one in the COMWIN system. This antenna has shown that its characteristics are similar to those of the standard antenna (a 4-foot-long whip antenna for 30 to 88 MHz, or a short-whip antenna for higher frequencies) used by the PRC-148 radios. Further investigation must be done to determine the effectiveness of the COMWIN vest antenna as a function of frequency, terrain, power level, and wearer orientation. Although several measurements were taken for the wearer in the prone position, the full effect of the change of impedance caused by the closeness of the ground must be investigated. Further research must be done for the test site in less mountainous terrain to determine the system's full range. Mountains restrict line-of-sight ranges.

The helmet antenna demonstrated the ability to receive video data at much higher frequencies than for which it was designed. The helmet antenna received video data at 2.4 GHz on an 802.11 protocol from a wireless LAN and displayed the data on a laptop computer. The helmet antenna increased the range from 30 to 160 m when compared to the microstrip antenna used on a conventional system. Further research into this should probably wait for the full investigation of the vest antenna. Measurements of the gain at frequencies from 400 to 1800 MHz show that the helmet antenna will be effective at most frequencies in this band.

The whole-body antenna is an effective receiver of signals in the 2- to 30-MHz band. The whole-body antenna received signals from station WWV at frequencies of 5, 10, 15, and 20 MHz. The reception quality was comparable, although lower than a 35-foot whip antenna. Further research will be needed to make the whole-body antenna capable of transmitting at power levels beyond 0.25 W. An inexpensive RF transformer used for efficient matching of the antenna to the feed restricts the power level. A new transformer must be fabricated that permits significant input power. This new transformer will be used to determine transmitter effectiveness and to perform radiation hazard experiments. Such a transformer will probably not be available until FY 2002.

The three antennas have now been integrated into a system. A switch on the wrist of the radio operator now directs the signal from the radio to one of three antennas for optimum transmission. The switch eventually will be directed by a data word input from the hand-held version of the Joint Tactical Radio. The word will be the result of entry of frequency and waveform by the radio operator. Further research into the integration must wait until the actual prototype of the radio is available (probably FY 2004).

The vest antenna has a severe radiation hazard for input power as high as 5 W. This problem must be solved before the vest antenna can be used safely. Fortunately, the solution appears to be straightforward. Material for simulating the dielectric and conductive properties of a person will be held next to the spots of significant radiation to shield the person from RF energy. This material will combine most of the best properties of ultra-wideband characteristics with the maximum in shielding. Safety of the wearer is the paramount issue. The first 3 months of FY 2002 will be devoted to solving this problem.

The COMWIN antenna system demonstrates the potential for ultra-wideband communication while disguising the radio operator. The basic design seems effective. Problems such as asymmetry between transmit and receive for some frequencies and radiation hazard can probably be solved by minor variations of the basic design. The thrust of research during FY 2002 will be to bring about a vest antenna that is safe and effective while achieving the above goals.

REFERENCES

- Adams, R. C., C. P. Haglind, H. Pace, J. Lebaric, R. Adler, T. M. Gainor, and A. T. Tan. 1999. "Fiscal Year 1999 Wideband Antenna Feasibility Study: Man-Carried Ultrawideband Antenna System," Technical Report 1808 (Nov), SSC San Diego, San Diego, CA.
- Adams, R. C., R. S. Abramo, J. L. Parra, and J. F. Moore. 2000. "COMWIN Antenna System Fiscal Year 2000 Report," Technical Report 1836 (Sep), SSC San Diego, CA.
- Chou, C. K., G. W. Chen, A. W. Guy, and K. H. Luk. 1984. "Formulas for Preparing Phantom Muscle Tissue at Various Radio Frequencies," *Bioelectromagnetics*, vol. 5, p. 435.
- Department of Defense, DODI 6055.11, February 21, 1995, "PEL (Permissible Exposure Limits) for Controlled Environments." 1995. DOD6055.11 (21 Feb), Washington, DC.
- Department of the Navy. 1999. "Non-Ionizing Radiation." OPNAVINST 5100.23E (15 Jan), Chapter 22, Washington, DC.
- Institute of Electrical and Electronics Engineers. 1991. "IEEE Standard for Safety Levels with Respect to Human Exposure to Radio Frequency Electromagnetic Fields, 3 kHz to 300 GHz," IEEE C95.1-1991, New York, NY.
- Mini-Circuits®. 1997. *RF/IF Designer's Handbook*. Brooklyn, NY.
- Operational Requirements Document (ORD) for Joint Tactical Radio (JTR). 1998. URL: http://www.fas.org/man/dod-101/sys/land/docs/jtr23_mar.htm.
- Thomas, T. 1999. "The Battle of Grozny: Deadly Classroom for Urban Combat," *Parameters*, vol. 29 (Summer), pp. 87-102.

INITIAL DISTRIBUTION

Defense Technical Information Center Fort Belvoir, VA 22060-6218	(4)	Marine Corps Warfighting Lab Quantico, VA 22134	
SSC San Diego Liaison Office C/O PEO-SCS Arlington, VA 22202-4804		Marine Corps Systems Command Quantico, VA 22134-5080	(5)
Center for Naval Analyses Alexandria, VA 22302-0268		Naval Health Research Center-Detachment Brooks AFB, San Antonio, TX	(2)
Office of Naval Research ATTN: NARDIC (Code 362) Arlington, VA 22217-5660		Naval Postgraduate School Monterey, CA 93943-5001	(2)
Government-Industry Data Exchange Program Operations Center Corona, CA 91718-8000		U.S. Army Communications-Electronics Command Fort Monmouth, NJ 07703-5027	(3)
Office of Naval Research Arlington, VA 22217-3127	(7)		
Space and Naval Warfare Systems Command San Diego, CA 92110-3127	(3)		
Space and Naval Warfare Systems Center North Charleston, SC 29419-9022	(3)		

Approved for public release; distribution is unlimited.